

RESEARCH ARTICLE

# iTRAQ-Based Quantitative Proteomics Analysis of Black Rice Grain Development Reveals Metabolic Pathways Associated with Anthocyanin Biosynthesis

Linghua Chen<sup>1,2</sup>, Yining Huang<sup>1,3</sup>, Ming Xu<sup>1,4</sup>, Zuxin Cheng<sup>1,4</sup>, Dasheng Zhang<sup>5,6</sup>, Jingui Zheng<sup>1,4\*</sup>

**1** Fujian Agriculture and Forestry University, Fuzhou Fujian, China, **2** Jinshan College of Fujian Agriculture and Forestry University, Fuzhou Fujian, China, **3** Department of Food and Biology Engineering, Zhangzhou Institute of Technology, Zhangzhou Fujian, China, **4** College of Crop Science, Fujian Agriculture and Forestry University, Fuzhou Fujian, China, **5** Shanghai Chenshan Plant Science Research Center, Shanghai Chenshan Botanical Garden, Chinese Academy of Sciences, Shanghai, China, **6** Shanghai Key Laboratory for Plant Functional Genomics and Resources, Shanghai, China

\* [jingui Zheng@126.com](mailto:jingui Zheng@126.com)



OPEN ACCESS

**Citation:** Chen L, Huang Y, Xu M, Cheng Z, Zhang D, Zheng J (2016) iTRAQ-Based Quantitative Proteomics Analysis of Black Rice Grain Development Reveals Metabolic Pathways Associated with Anthocyanin Biosynthesis. PLoS ONE 11(7): e0159238. doi:10.1371/journal.pone.0159238

**Editor:** Tai Wang, Institute of Botany, Chinese Academy of Sciences, CHINA

**Received:** March 29, 2016

**Accepted:** June 29, 2016

**Published:** July 14, 2016

**Copyright:** © 2016 Chen et al. This is an open access article distributed under the terms of the [Creative Commons Attribution License](https://creativecommons.org/licenses/by/4.0/), which permits unrestricted use, distribution, and reproduction in any medium, provided the original author and source are credited.

**Data Availability Statement:** All relevant data are within the paper and its Supporting Information file.

**Funding:** This work was supported by the National Key Technology R&D Program (2013BAD01B05) and the Science and Technology Innovation Platform Development Program of Fujian Agriculture and Forestry University (PTJH13001, PTJH12015).

**Competing Interests:** The authors have declared that no competing interests exist.

## Abstract

### Background

Black rice (*Oryza sativa* L.), whose pericarp is rich in anthocyanins (ACNs), is considered as a healthier alternative to white rice. Molecular species of ACNs in black rice have been well documented in previous studies; however, information about the metabolic mechanisms underlying ACN biosynthesis during black rice grain development is unclear.

### Results

The aim of the present study was to determine changes in the metabolic pathways that are involved in the dynamic grain proteome during the development of black rice *indica* cultivar, (*Oryza sativa* L. *indica* var. SSP). Isobaric tags for relative and absolute quantification (iTRAQ) MS/MS were employed to identify statistically significant alterations in the grain proteome. Approximately 928 proteins were detected, of which 230 were differentially expressed throughout 5 successive developmental stages, starting from 3 to 20 days after flowering (DAF). The greatest number of differentially expressed proteins was observed on 7 and 10 DAF, including 76 proteins that were upregulated and 39 that were downregulated. The biological process analysis of gene ontology revealed that the 230 differentially expressed proteins could be sorted into 14 functional groups. Proteins in the largest group were related to metabolic process, which could be integrated into multiple biochemical pathways. Specifically, proteins with a role in ACN biosynthesis, sugar synthesis, and the regulation of gene expression were upregulated, particularly from the onset of black rice grain development and during development. In contrast, the expression of proteins related to signal transduction, redox homeostasis, photosynthesis and N-metabolism decreased during grain maturation. Finally, 8 representative

genes encoding different metabolic proteins were verified via quantitative real-time polymerase chain reaction (qRT-PCR) analysis, these genes had differed in transcriptional and translational expression during grain development.

## Conclusions

Expression analyses of metabolism-related protein groups belonging to different functional categories and subcategories indicated that significantly upregulated proteins were related to flavonoid and starch synthesis. On the other hand, the downregulated proteins were determined to be related to nitrogen metabolism, as well as other functional categories and subcategories, including photosynthesis, redox homeostasis, tocopherol biosynthetic, and signal transduction. The results provide valuable new insights into the characterization and understanding of ACN pigment production in black rice.

## Introduction

Rice (*Oryza sativa* L.) is one of the primary cereals of the world, serving as a major staple food source to more than half of the global population [1]. The most commonly consumed rice type is white rice; however, several special cultivars of rice consist of colored pigments such as red and black. Black rice presents a dark purple color, which is due to its high anthocyanin (ACN) content that is mainly secreted in the pericarp [2–4]. Black rice has been historically considered as a highly nutritious food in China and other East Asian countries [5]. Today, black rice is becoming increasingly popular in the US, Australia, as well as Europe, particularly in terms of its health benefits.

ACNs pertain to water-soluble flavonoids and are the primary pigments of black and red grains, as well as various other fruits, vegetables, cereals, and flowers [6]. In plants, ACNs serve as pollinators and seed dispersers, as well as photoprotectants that scavenge free radicals that are generated during photosynthesis [7]. Recent interest in ACNs as health-promoting food ingredients has mainly been due to its reported antioxidant activity [8, 9], which may contribute to the prevention of chronic and degenerative diseases [10–13]. Previous reports have also shown that ACNs also possess anti-inflammatory properties prevent arteriosclerosis [14] and hyperlipidemia [15, 16], lower glycemic indices [17], promote visual acuity [18], and hinder obesity and diabetes [19]. In addition, animal studies showed that an ACN-rich extract derived from black rice showing a relatively high ACN content (43.2%) imparted similar effects [20].

The involvement of ACNs in various important functions poses questions on how these compounds are produced, as well as regulated. In the past 3 decades, intensive studies have improved our understanding of ACNs in plant biology, including the biosynthesis and regulation of ACNs with other metabolites in various plant species such as *Arabidopsis* [20], maize [21], grape [22], orange [23], and apple [24], and majority of these ACN biosynthesis genes of interest has been cloned [25–28]. However, the synthesis of ACNs in black rice remains poorly understood and rarely studied despite its classification as a model crop plant and its genome being completely sequenced [29]. Furthermore, certain cultivars that contain high levels of ACNs have been developed, and these efforts facilitate in better understanding the activities relating to this particular biosynthetic pathway in black rice. Cyanidin-3-glucoside (C3G) and peonidin-3-glucoside (P3G), which are the predominant pigments in black rice, are the most powerful among the 14 main ACNs [30–33]. The cultivar (cv.) Heugjinju has the highest ACN and C3G levels among the dark purple rice cultivars [3, 29, 34].

Proteomics studies are generally conducted to obtain a comprehensive evaluation of proteins that respond to a specific environment or treatment, and these investigations provide both quantitative and active information, and protein-protein interactions[35]. Proteomic analysis of rice grains was previously reported, and the protein spots were identified by mass spectrometry as 309[36], 298[37], and 54[38], respectively. However, these investigations were performed using gel-based techniques, which limits the detection of proteins within grain proteomes. One disadvantage of this gel-based procedure is that the markedly over-represented group of grain-specific proteins may mask low-level proteins, thereby rendering its detection difficult [39]. Moreover, membrane proteins with several membrane spanning domains are difficult to detect on classical two-dimensional electrophoresis (2-DE) gels due to its low abundance as well as poor solubility in aqueous media[40]. The recently developed isobaric tags for relative and absolute quantitation (iTRAQ) proteomic method allow the unbiased and simultaneous observation of relative protein abundances within a cell during harvest [41–43]. Therefore, the iTRAQ method is suitable for investigating proteomic changes under various developmental processes[44]. iTRAQ was recently utilized in plant fruit development research of wheat [45] and grape[46–48]. Interestingly, iTRAQ has been determined to be a potentially useful approach in rice grain development research, as indicated by the results of a recent study on the mechanistic responses of inferior spikelets to drought stress [49].

In the present study, iTRAQ was utilized in the proteomic analysis of black rice grain to reveal the unique genetic profile, as well as identify alterations in the levels of protein expression during development. The goal of this study was to reveal differentially expressed proteins at five time points during the development of black rice grains (*O. sativa* L. *indica* var. SSP), as well as compare these protein expression patterns to identify candidate proteins that may be potentially involved in ACN biosynthesis. Furthermore, specific proteins were selected to correlate whether alterations in protein expression may be validated using transcript analysis. The results of the present study provide global insights into proteome modifications in black rice during development.

## Materials and Methods

### Plant materials and sampling

Black rice (*O. sativa* L. *indica* var. SSP) plants were cultured during the rice growing season (May to September) under natural and normal field conditions at the Fujian Agriculture University experimental field and were fertilized (urea, 60 kg/ha) using routine procedures. In rice, developing seeds are categorized as superior or inferior based on its location on spikes[50]. The superior seeds, which are located at the topmost region of the spike, generally show a higher growth rate, as well as simultaneously reach maturity. Therefore, in the present study, superior seeds were selected as experimental samples based on its distinguishing advantage of synchronous development [36]. The superior seeds of the topmost 3 spikelets were then labeled at noon during anthesis, when at least 50% of the superior seeds belonging to the corresponding spikelets were at the flowering stage[50]. The labeled spikelets were thus harvested at 2, 3, 5, 7, 10, 13, 15, 17, and 20 days after flowering (DAF). After being dehusked, samples from each of these stages comprised at least 200 seeds derived from 30 spikes that were immediately stored at -80°C until protein extraction.

### Total anthocyanin content (TAC) measurement

The reported spectrophotometric method with some modifications was used to determine the total amount of ACNs[51]. Briefly, the seeds were ground to a fine powder in liquid nitrogen. Approximately 3 g of the powder was transferred into a 50mL tube, and then a total of 24 mL

of acidified ethanol (ethanol and 1.0 N HCl, 85:15, v/v) was then added for total anthocyanin content extraction. The solution was then mixed and adjusted to a pH level of 1 using 4 N HCl. The resulting solution was then shaken for 15 min, readjusted to pH 1 as required, and then again shaken for another 15 min. The tube was then centrifuged at 30,000g for 15 min, and the supernatant was transferred into a 50-mL volumetric flask, and acidified ethanol was added to top up to volume. Triplicate biological preparations were performed for each sample. Absorbance was measured at a wavelength of 535 nm against a blank. The TAC (in micrograms per gram) was calculated as follows:

$$\text{TAC} = A \times 28.82;$$

where  $A$  is the absorbance reading [51].

### Protein extraction and digestion

Seeds (1 g) were ground in ice-cold extraction buffer [20 mM Tris-HCl (pH 8.0), 20 mM NaCl, 10 mM phenylmethylsulfonyl fluoride, and 10 mM dithiothreitol]. The supernatant was separated by centrifugation at 35,000g for 20 min at 4°C. The pellet was then resuspended in fresh extraction buffer for another round of extraction, and then again centrifuged at 35,000g for 20 min at 4°C to separate the supernatant. The proteins in the pooled supernatants were precipitated using 4 volumes of ice-cold trichloroacetic acid-acetone (10% trichloroacetic acid mixed in 100% acetone) for 4 h at -20°C, followed by isolation via centrifugation at 35,000g for 20 min. The protein pellet was then washed with cold 80% acetone with 0.07% (w/v)  $\beta$ -mercaptoethanol, followed by cold acetone with 0.07% (w/v)  $\beta$ -mercaptoethanol, and then vacuum-dried as previously elsewhere [52]. The homogenate was then centrifuged, and the collected pellets were air-dried, mixed in 800  $\mu$ L STD buffer (4% SDS, 150 mM Tris-HCl, 100 mM DTT, pH 7.6), boiled for 5 min, and then sonicated. After centrifugation, the supernatants were then collected, and protein content was measured by using a BCA protein assay reagent (Beyotime Institute of Biotechnology, Shanghai, China). Similar amounts of proteins (120  $\mu$ g from 3, 7, 10 DAF, 15, and 20 DAF) were then mixed and used as reference (REF).

Protein digestion was conducted using the FASP procedure [53]. For each sample, 300  $\mu$ g of proteins were placed on an ultrafiltration filter (30 kDa cut-off, Sartorius, Gottingen, Germany) that consisted of 200  $\mu$ L of UA buffer (8 M urea, 150 mM Tris-HCl, pH 8.0), centrifuged at 14,000g for 30 min, and then washed using 200  $\mu$ L of UA buffer. Approximately 100  $\mu$ L of 50 mM iodoacetamide was then added to the filter in order to block any reduced cysteine residues. The samples were then kept at room temperature for 30 min in the dark, which was followed by centrifugation at a speed of 14,000g for 30 min. The filters were then washed twice with UA buffer (100  $\mu$ L), followed by centrifugation at 14,000g for 20 min after every wash. Next, approximately 100  $\mu$ L of a dissolution buffer (Applied Biosystems, Foster City, CA, USA) was placed on the filter, and then centrifuged at 14,000g for 20 min, and then repeated twice. Then, the protein suspensions were subjected to enzyme digestion using 40  $\mu$ L of trypsin (Promega, Madison, WI, USA) buffer (4  $\mu$ g trypsin in 40  $\mu$ L of dissolution buffer) for 16–18 h at 37°C. Last, the filter unit was then transferred to a new tube and spun at 14,000g for 30 min. The collected peptides were collected in the form of a filtrate, and the concentration of the peptides was analyzed at an optical density using a wavelength of 280 nm ( $\text{OD}_{280}$ ) [53].

### iTRAQ labeling and strong cation exchange

iTRAQ labeling was conducted following the manufacturer's recommendations (Applied Biosystems, Foster City, CA, USA). Briefly, the peptide pellet was reconstituted in 30  $\mu$ L of the iTRAQ dissolution buffer. Labeling of each sample (100  $\mu$ g) using the iTRAQ Reagent-8plex

Multiplex Kit (AB SCIEX, Framingham, MA, USA) at 3, 7, 10, 15, and 20 DAF samples was performed twice. A REF sample was then added to each group. Then, the labeling reaction was kept at room temperature for 1 h before further analysis. From each group, 7 labeled samples were pooled and then vacuum-dried in a centrifuge at room temperature.

The iTRAQ-labeled peptides were then subjected to the procedure of strong cation exchange fractionation using an AKTA Purifier 100 (GE Healthcare, Little Chalfont, Bucks, UK), which was equipped with a polysulfethyl (PolyLC Inc., Columbia, MD, USA.) column (4.6 mm × 100 mm, 5 μm, and 200 Å). The peptides were then eluted at a flow rate of 1 mL/min. Buffer A comprised 10 mM KH<sub>2</sub>PO<sub>4</sub> and 25% v/v can (pH 3.0), whereas Buffer B contained 10 mM KH<sub>2</sub>PO<sub>4</sub>, 25% v/v ACN, and 500 mM KCl (pH 3.0). Both buffers were then filter-sterilized. The gradient utilized for separation was as follows: 100% Buffer A for 25 min, 0–10% Buffer B for 7 min, 10%–20% Buffer B for 10 min, 20%–45% Buffer B for 5 min, 45%–100% Buffer B for 5 min, 100% Buffer B for 8 min, and lastly, 100% Buffer A for 15 min. Monitoring of the elution process was performed by measuring the absorbances at a wavelength of 214 nm, with fractions collected at 1-min intervals. The collected fractions (a total of 30) were then combined into 10 pools and desalted using C18 cartridges (Sigma, Santa Clara, CA, USA). Every fraction was concentrated by vacuum centrifugation, followed by reconstitution in 40 μL of 0.1% (v/v) trifluoroacetic acid. The samples were stored at -80°C until LC-MS/MS analysis.

### LC-MSMS analysis

The iTRAQ-labeled samples were then analyzed by using the Easy-nLC nanoflow HPLC system (Thermo Fisher Scientific, Karlsruhe, BW, Germany), which was connected to an LTQ Orbitrap Elite mass spectrometer (Thermo Fisher Scientific, Karlsruhe, BW, Germany). A total of 1 μg of every sample was loaded onto an Thermo Scientific EASY column (two columns) using an autosampler, using a flow rate of 150 nL/min. Peptide sequential separation using the Thermo Scientific EASY trap column (100 μm × 2 cm, 5 μm, 100 Å, C18) and analytical column (75 μm × 25 cm, 5 μm, 100 Å, C18) was conducted using a segmented 2-h gradient of Solvent A (0.1% formic acid in water) to 35% Solvent B (0.1% formic acid in 100% ACN) for 100 min, which was then followed by 35%–90% Solvent B for 3 min, and finally, 90% Solvent B for 5 min. Then, the column was re-equilibrated to attain its initial highly aqueous solvent composition prior to analysis.

The mass spectrometer was run in a positive ion mode, wherein the MS spectra were acquired within a range of 300–2,000 m/z. The resolution of the MS and MS/MS scan using 200 m/z for the LTQ Orbitrap Elite was set to 60,000 and 15,000, respectively. The 10 signals showing the highest intensities in the acquired MS spectra were then selected for additional MS/MS analysis. The isolation window employed was 1 m/z, with ions fragmented using higher energy collisional dissociation at normalized collision energies of 35 eV. The highest ion injection times utilized were 50 ms for the survey scan and then 150 ms for the MS/MS scans, whereas the automatic gain control target values for the full scan modes were set to  $1.0 \times 10^{-6}$ , and that for MS/MS was  $5.0 \times 10^4$ . The dynamic exclusion duration was 30 s.

### Database search and protein quantification

The raw files were analyzed by using the software, Proteome Discoverer 1.4 (Thermo Fisher Scientific, Karlsruhe, BW, Germany). Identification of the fragmentation spectra was conducted using the MASCOT 2.2 search engine that was embedded in Proteome Discoverer and run against the rice protein database (released in May 2015 and including 144,386 sequences from NCBI). The search parameters were as follows: monoisotopic mass, trypsin utilized as the cleavage enzyme, two missed cleavages, iTRAQ labeling and carbamidomethylation of cysteine

used as fixed modifications; and peptide charges of 2+, 3+, and 4+, as well as methionine oxidation were designated as variable modifications. The mass tolerance was 10 ppm for precursor ions and 0.05 Da for fragmented ions. The results were then filtered according to a false discovery rate (FDR) of <1%.

The relative quantitative protein analysis of samples according to the ratios of iTRAQ reporter ions derived from all unique peptides that represented each protein was conducted using the Proteome Discoverer software (version 1.4). The relative peak intensities of the iTRAQ reporter ions that were derived from each of the MS/MS spectra were employed, and the REF sample was used as a reference in calculating for the iTRAQ ratios of the reporter ions. The final ratios derived from the relative protein quantifications were then normalized according to the median protein quantification ratio. The protein ratios represented the median of the unique peptides in the protein. Only proteins identified at all two replicates were considered for further analysis.

### Bioinformatics functional analysis

Statistical and hierarchical clustering analyses were performed using Perseus V1.4.1.3 ([http://141.61.102.17/perseus\\_doku/](http://141.61.102.17/perseus_doku/)) [54, 55]. P-values < 0.05 by Benjamini-Hochberg FDR in Perseus and a ratio fold-change of >1.20 or <0.83 in expression between any two groups were considered significant. The hierarchical clustering analysis was performed using the following settings: Row, Column distance that was calculated using the Euclidean algorithm; Row, Column linkage-Complete. Functional analysis of the identified proteins was performed using Gene Ontology (GO) annotation (<http://www.geneontology.org>), and the proteins were categorized based on its biological process, molecular function, as well as cellular localization [56]. The differentially expressed proteins were then further assigned to the Clusters of Orthologous Groups of proteins (COG) database (<http://www.ncbi.nlm.nih.gov/COG/>) [57].

### RNA extraction and qRT-PCR analysis

Total RNA was extracted from leaves by using the TaKaRa RNAiso reagent (TaKaRa Bio, Otsu, Japan) and then treated with RNase-free DNase I (TaKaRa Bio, Otsu, Japan) [58]. The purified RNA was reverse-transcribed by using the M-MLV reverse transcription system (Promega, Madison, WI, USA), following the manufacturer's instructions. qRT-PCR was conducted in 96-well blocks using an CFX96 Real-time System (BioRad, Hercules, CA, USA) using the SYBR Green I master mix in a volume of 25  $\mu$ L. Each qRT-PCR was run in triplicate. To normalize the expression data, the gene, *Actin* (GenBank Accession Number: AY212324) was used as internal reference. Relative expression levels were then calculated by using the  $2^{-\Delta\Delta CT}$  (cycle threshold) method [59].

## Results

### Physiological characterization of developing black rice grains

To generate basic information on rice seed development, we examined the morphological features as well as dynamic changes in reserve accumulation in the developing seeds at 2, 3, 5, 7, 10, 13, 15, 17, and 20 DAF (Fig 1A and 1B). The developing seeds showed a significant increase in size starting from 2 to 7 DAF, followed by a slight increase that apparently reached the size of mature seeds at around 13 DAF (Fig 1A). After 17 DAF, the seeds became black and full-filled (Fig 1A). On the other hand, both fresh and dry weights apparently changed insignificantly from 2 to 7 DAF, although these rapidly increased thereafter up to 17 DAF (Fig 1B). Beyond 17 DAF, the increase in dry weight occurred at a slower rate, although the fresh weight

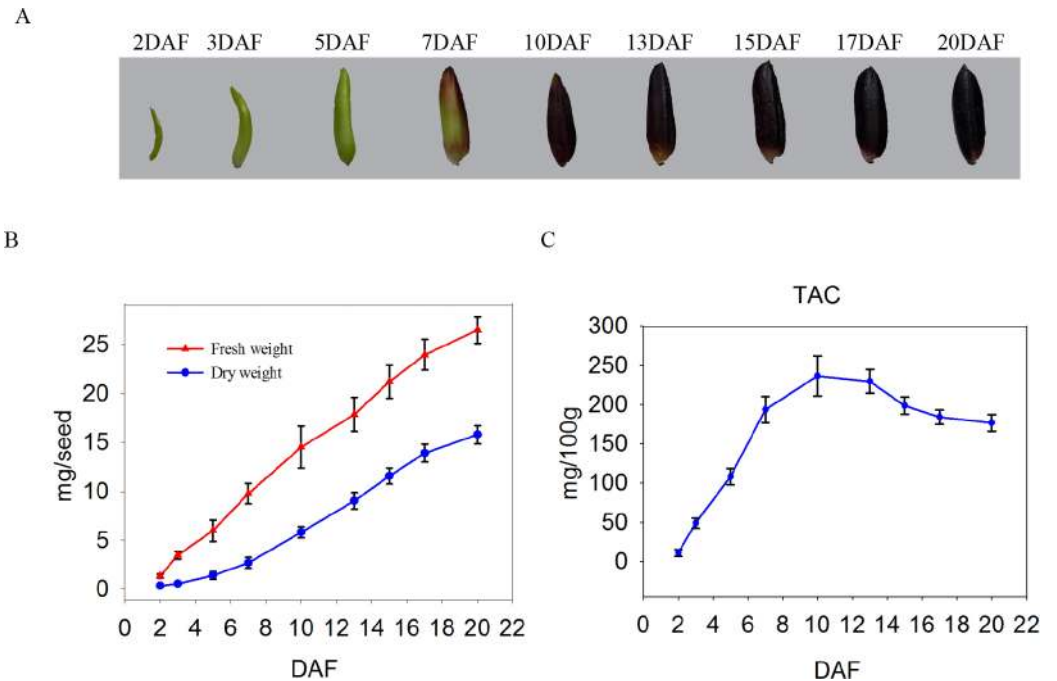


**Fig 1. Development of black rice seed.** (A) The 9 stages of seed development. (B) Changes in the fresh and dry weights of developing seeds. At least 100 seeds were examined at various stages of development. (C) Changes in total anthocyanin content (TAC) levels in developing seeds.

doi:10.1371/journal.pone.0159238.g001

continued to increase until 20 DAF, thereby indicating that the developing seeds had entered the desiccation phase by 17 DAF. The developmental alterations in seed size, fresh weight, as well as dry weight were generally similar with the results of previous investigations [32, 60]. Taken together, the results of the present study indicate that developing seeds up to 7 DAF are actively dividing and differentiating, and the grains begin to fill and then ripen at 7 DAF, which then continues on up to 20 DAF. Because the goal of the present study was to conduct protein expression profiling in relation to ACN biosynthesis during grain filling, we determined the dynamic change in the TAC in seeds. The results indicated that TAC content increased from 2 to 10 DAF, which was then followed by a dramatic decrease (Fig 1C), thereby suggesting 2 points: (1) ACNs did not accumulate during the early stages and the grains appeared almost non-pigmented, and (2) the rates of development of the bran outer layers and endosperm differ because ACNs exist almost exclusively at the early and mid-stages, but not at the late stages. Based on these observations, we then divided the development process encompassing 2 to 20 DAF into early (2–7 DAF), mid (7–13 DAF), and late (13–20 DAF) categories, and used the developing seeds at 3, 7, 10, 15, and 20 DAF for further analysis.

### General information on iTRAQ analysis

In the present study, a total of 2,084 proteins were identified in the experiments, which included the developmental stages and replicates of the iTRAQ proteomic analysis. Approximately 928 proteins were identified in the 2 biological replicates and were subsequently included in a comparative analysis. Fig 2 shows the basic information that was generated from the iTRAQ-LC-MS/MS data. The molecular weights of majority of the identified proteins (80%, Fig 2A) were between 20 and 70 kDa. The distribution analysis of the sequence

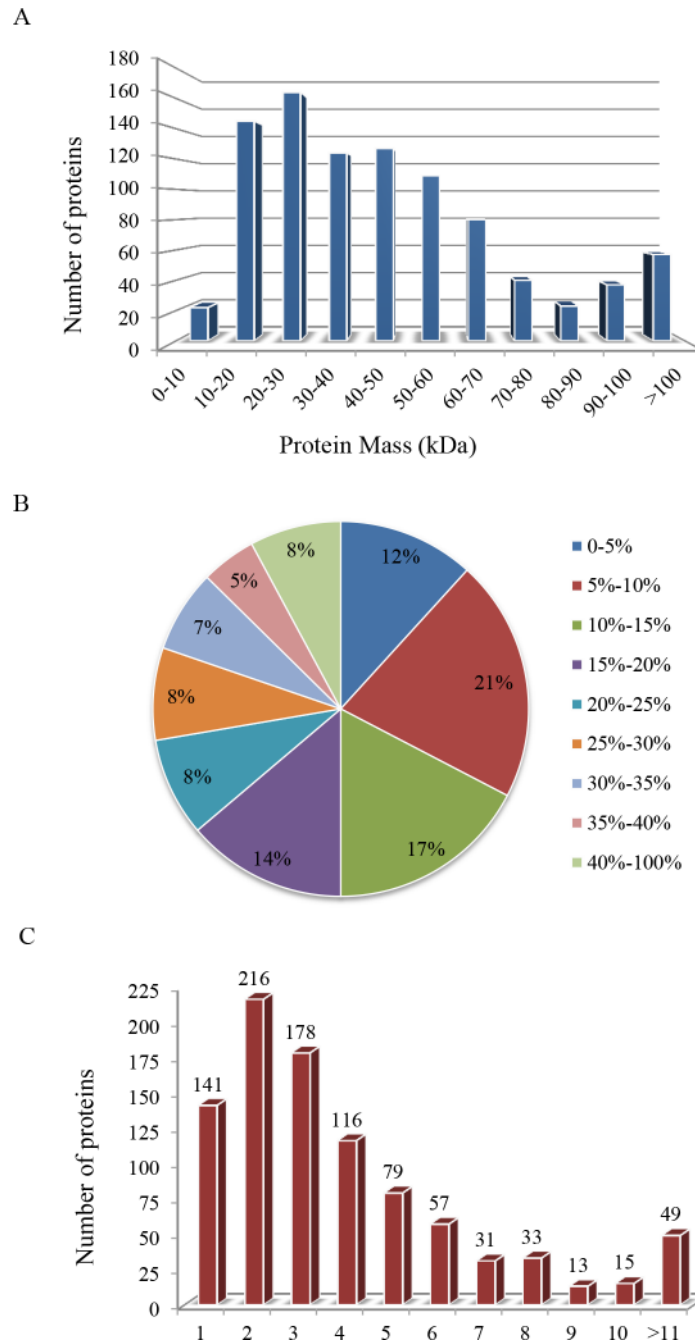


**Fig 2. General information on the iTRAQ-LC-MS/MS analysis that was performed using black rice seed.** (A) Distribution of proteins of different molecular weights. (B) Coverage of proteins by using LC-MS/MS-identified peptides. (C) Unique peptides of the detected proteins. The number of proteins in each of the categories is presented above each bar.

doi:10.1371/journal.pone.0159238.g002

coverage of the detected peptides indicated that 88% of these proteins have a coverage that was >5% (Fig 2B) and that 84.81% (787) were inferred from at least 2 unique peptides (Fig 2C). These results thus indicate good quality data.



### Comparative analysis of protein expression at five developmental stages

Using a cutoff of P-value <0.05 and a ratio fold-change of >1.20 or <0.83 for expression, we identified 230 differentially expressed proteins after comparing at least 1 sample pair (S1 Table). These 230 proteins were grouped based on fold-change in expression, as visualized in Fig 3. The analysis revealed 2 main branches. DAF 3 was distinct from DAF 7, 10, 15, and 20. Similarly, DAF 7, 10, 15, and DAF 20 were also distinguishable from each other, and could be resolved into 2 separate clusters within the same branch. The maximum number of differentially expressed proteins was observed in the sample pair consisting of the time points of 7 and 10 DAF (76 upregulated and 39 downregulated proteins), followed by the sample pair made up of the time points of 10 and 15 DAF (77 unregulated and 28 downregulated proteins) (Fig 4). This finding indicates that a distinct metabolic phase could possibly serve as an indicator of

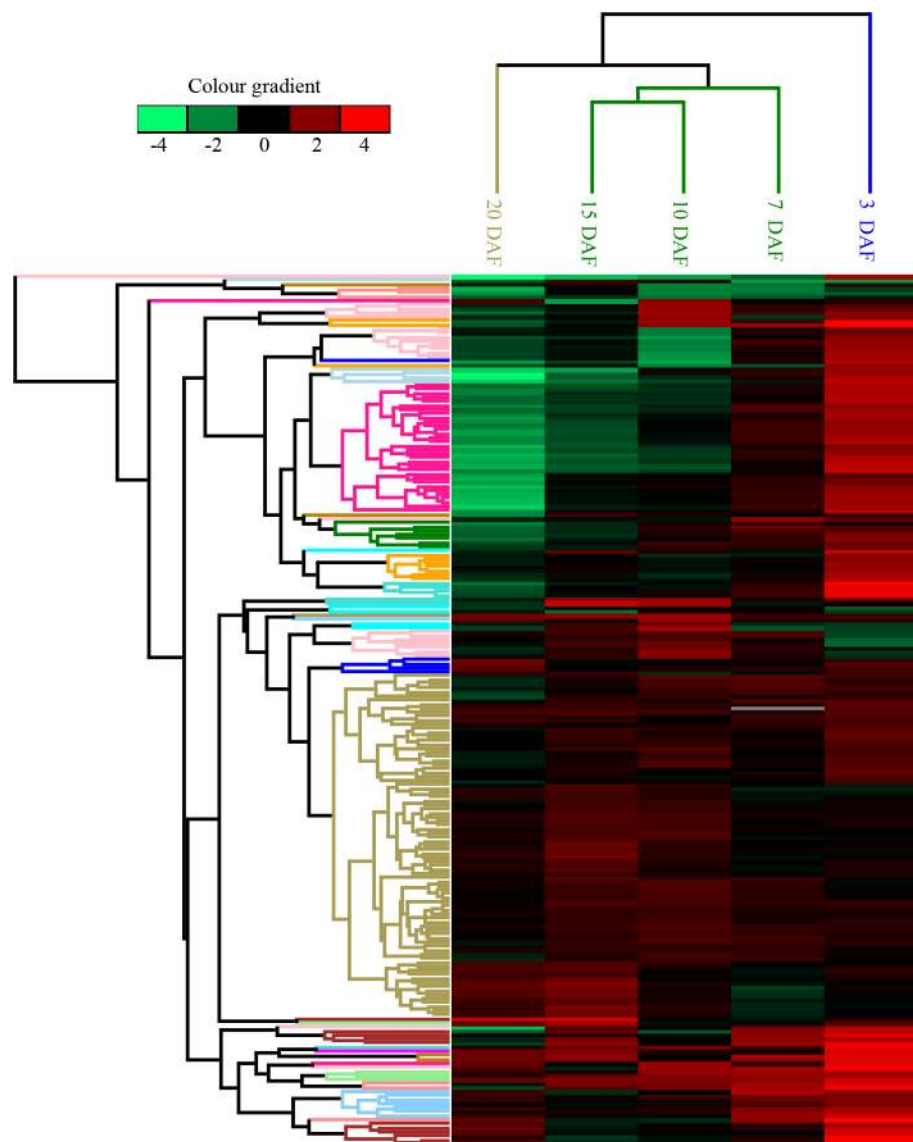


**Fig 3. Hierarchical clustering analysis of the 230 differentially expressed proteins at 5 seed development stages.** Green: Reduced expression compared to that observed in the REF. Red: Increased expression compared to that detected in the REF. White: No data.

doi:10.1371/journal.pone.0159238.g003

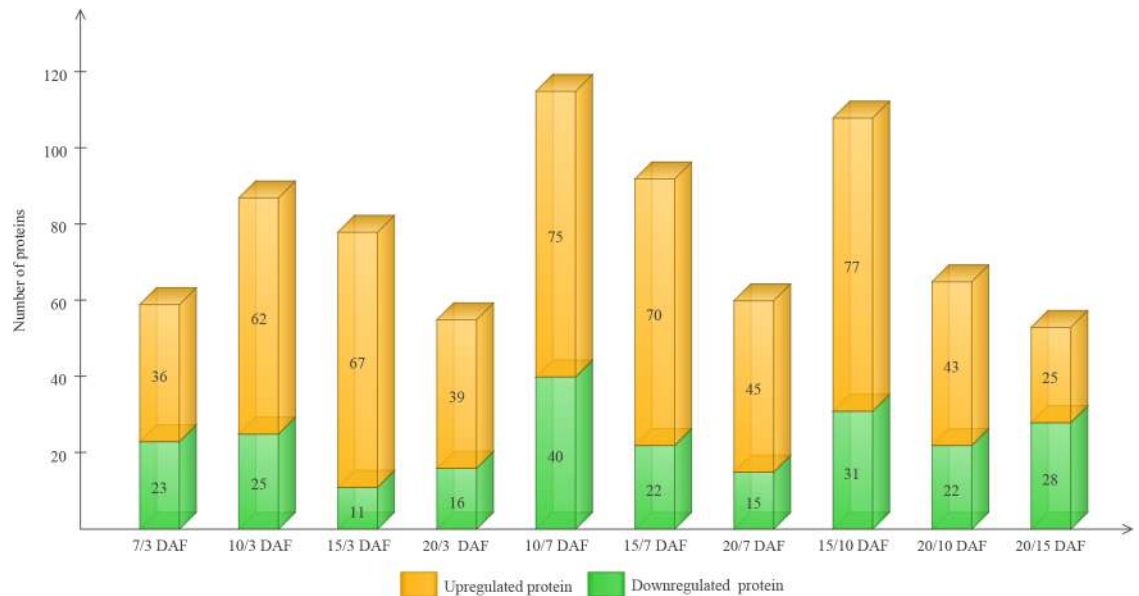


**Fig 4. The number of differentially expressed proteins in 5 seed development stages.** The x-axis indicates the comparisons between any two samples. The left y-axis shows the number of differentially expressed proteins.

doi:10.1371/journal.pone.0159238.g004

developmental reprogramming. In contrast, the sample pair consisting of the time points of 15 and 20 DAF presented the lowest number of differentially expressed proteins (25 upregulated and 28 downregulated proteins) (Fig 4), which may be attributable to the low level of metabolic activity in cells during grain development.

**Classification of metabolic process-specific proteins.** The 230 differentially accumulated proteins were categorized into 3 groups (biological process, cellular component, and molecular function) based on the results of GO analysis. According to the biological process properties (Fig 5), the main functional categories were metabolic process (26.09%), cellular process (24.38%), response to stimulus (9.95%), localization (4.98%), establishment of localization (4.98%), cellular component organization (3.48%), pigmentation (3.48%), cellular component biogenesis (3.48%), biological regulation (3.48%), anatomical structure formation (2.99%), immune system process (2.49%), multicellular organismal process (1.99%), developmental process (1.0%), and multi-organism process (0.5%). The most represented GO term was ‘metabolic processes’, with 60 proteins differentially regulated during black rice grain development. Through KEGG (<http://www.kegg.jp/>), Metacyc (<http://metacyc.org/>), and UniPathway (<http://www.grenoble.prabi.fr/obiwarehouse/unipathway>) analyses, as well as a review of literature indicated that the 60 differentially expressed proteins of the metabolic process GO category were assigned to 9 subgroups (Fig 6).

### Validation using quantitative RT-PCR

To validate the quantitative results relating to the correspondence between proteins and its mRNA expression patterns, 8 metabolic process proteins were performed to evaluate the dynamic transcriptional expression profiles by using quantitative RT-PCR (Q-PCR) analysis. The relatively high amplification efficiency of every primer pair was designed using the software, primer-BLAST[61], and the sequences are presented in Table 1. Fig 7 shows that 2 genes encoding chalcone synthase 1 (CHS) and methylthioribose-1-phosphate isomerase (M1P1) displayed similar protein expression patterns, and four genes encoding sucrose synthase 4

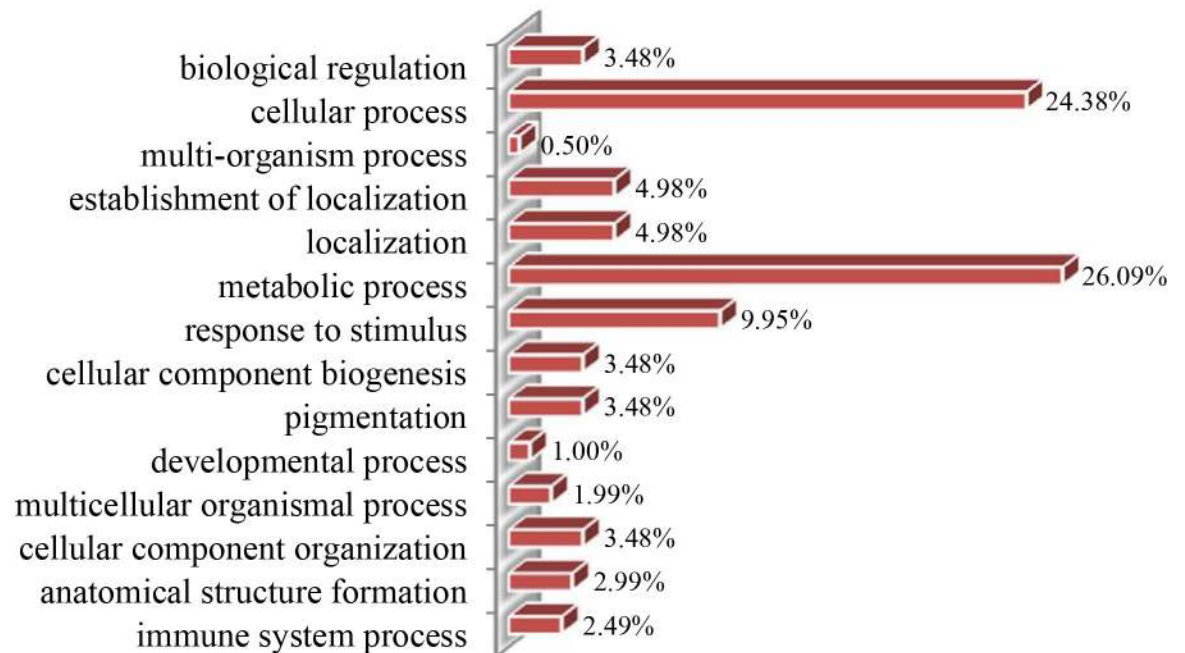


**Fig 5. Biological process classification of differentially accumulated proteins during grain development.**

doi:10.1371/journal.pone.0159238.g005

(SUS4), Ras-related protein RIC2(RAP), phosphoribulokinase (PRK), and phosphoribulokinase (ALT) showed expression patterns at 5 developmental stages that were similar to its protein expression profiles. On the other hand, 2 genes encoding elongation factor 1-delta 2 (EF-1δ1) and 40S ribosomal protein S8 (40S RPS8) showed expression patterns that were opposite to that of its proteins. The mRNA and protein levels of EF-1δ1 and 40S RPS8 differed and may be attributable to translational or post-translational modifications.

## Discussion

The pericarp of black rice seeds consists of high levels of ACN. However, information regarding metabolic mechanisms underlying ACN biosynthesis is limited. In the present study, iTRAQ-based quantitative proteome analysis indicated the occurrence of dynamic changes in metabolic process proteins of black rice seeds at 5 developmental stages. The number of identified metabolic proteins was significantly higher than that observed in previous reports using traditional gel-based approaches [36, 62, 63]. These metabolic proteins were mainly involved in C-metabolism, N-metabolism, as well as the flavonoid biosynthesis pathway.

## Proteins involved in signal transduction

Black rice grains perceive ACN biosynthesis signals by using putative sensors, which are then transmitted to the cellular machinery via signal transduction in order to regulate gene expression. Two proteins involved in signal transduction were detected and quantified in the present study, namely, mitochondrial Rho GTPase (Rho GTPase) and Ras-related protein RIC2 (RAP). These findings suggest that the Rho family GTPases, as well as RAP act as key molecular switches that control a variety of actin-based cellular processes, including the establishment of cell polarity, cellular morphogenesis, and motility of diverse eukaryotic organisms [64]. Rho GTPase and RAP were upregulated at 3 DAF and were downregulated during rice grain ripening (Fig 8A). The observed changes in the characteristics of these 2 proteins and the TAC



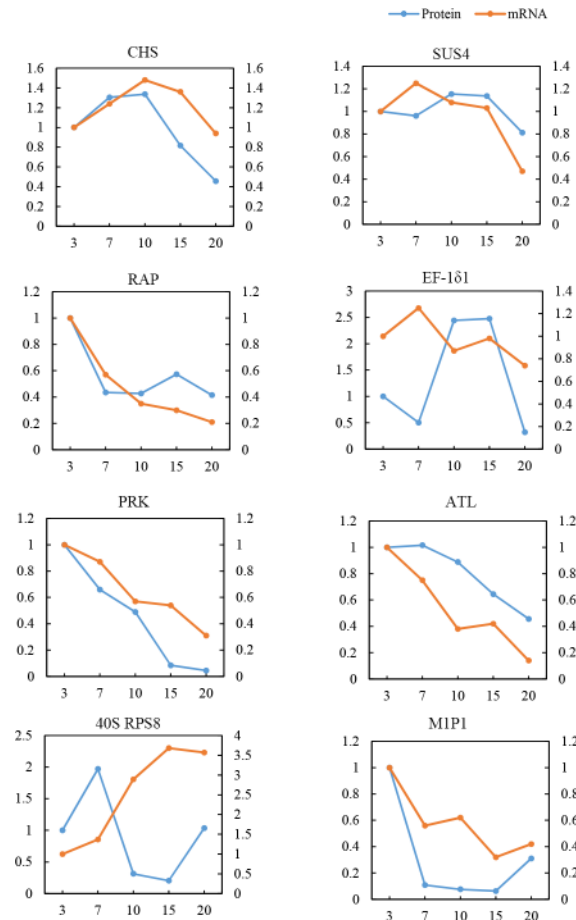


**Fig 7. Comparative analysis of protein and mRNA profiles of 8 representative metabolic proteins.** The x-axis represents days after flowering (DAF). The left y-axis indicates the relative protein level, whereas the right y-axis pertains to the relative mRNA level. The blue line represents the pattern of protein expression, and the orange line indicates the pattern of mRNA expression.

doi:10.1371/journal.pone.0159238.g007

eukaryotic translation initiation factor 3 subunit C (eIF3C), 40S ribosomal protein S7(40S RPS7) and S8(40S RPS8), and 60S acidic ribosomal protein P0 (60S RPLP0) were all involved in the translation and processing of proteins. These findings suggest that eukaryotic elongation factors (eEFs) are involved in the translation elongation cycle, which deliver aminoacyl-tRNAs (aa-tRNAs) to the elongation ribosome. Although EF-1 $\gamma$ , eIF3C, and 60S RPLP0 were downregulated (Fig 8B), EF-1 $\delta$ 1, EF-1 $\delta$ 2, 40S RPS7, and 40S RPS8 were upregulated during DAF10,15,10, and7, respectively (Fig 8C). The differential regulation of various components of the translation machinery is indicative of a complicated mechanism of controlling protein synthesis during grain development. Heat shock proteins function in minimizing the aggregation of newly synthesized proteins, thereby facilitating the folding process [67]. Heat shock protein 90 (HSP90) was downregulated during grain development (Fig 8D), which in turn may play a critical role in preventing clumping of denatured proteins and in facilitating protein refolding during grain development. In plants, post-transcriptional gene silencing (PTGS) involves the reduction in the levels of specific RNAs upon the introduction of homologous sequences into the plant genome. This particular reduction is due to an increase in turnover of target RNA species, while transcription levels of corresponding genes are unaltered [68]. In the present study, a protein suppressor of gene silencing 3 (SGS3) was identified

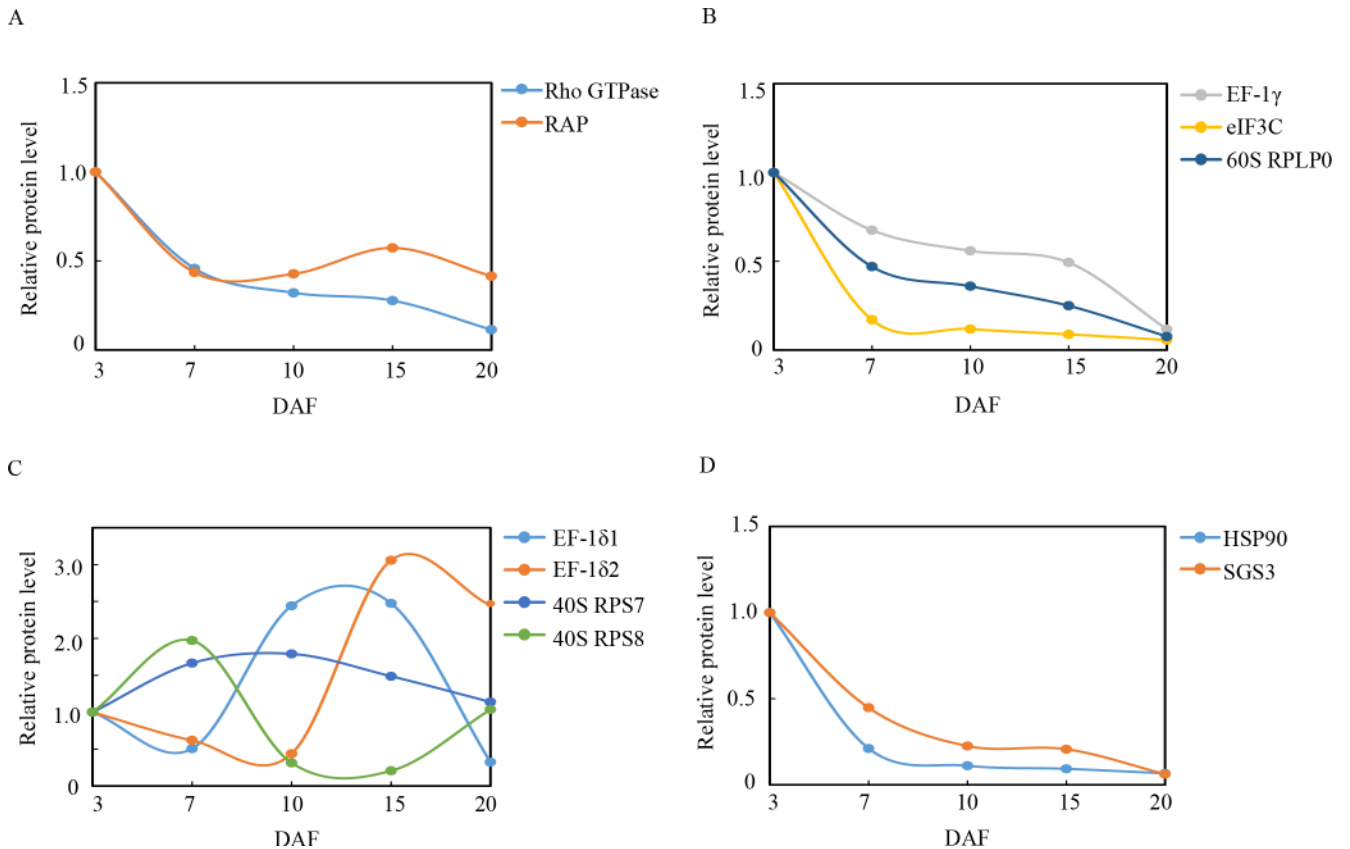


**Fig 8. Relative expression patterns of signal transduction, as well as gene expression regulation proteins during grain development.** The expression level was established in relation to 3 days after flowering (DAF) (vertical axis) at various developmental stages (horizontal axis, DAF).

doi:10.1371/journal.pone.0159238.g008

and quantified, which was downregulated during rice grain development (Fig 8D). However, the role of SGS3 in rice grain development remains elusive.

### Proteins involved in redox homeostasis

Redox homeostasis pertains to the metabolic interface that links stress perception with physiological responses [69]. Previous studies have shown that the early signaling events that control transcription factor expression, which in turn coordinates and regulates the entire flavonoid biosynthesis pathway, are redox-sensitive [70]. Plants regulate redox homeostasis using sophisticated mechanisms, including scavenging radicals by using peroxidases, (i.e., catalase, peroxidase 2, and class III peroxidase 122) and a nucleoside diphosphate kinase (NDPK), which were all identified in the present study. Nucleoside diphosphate kinase (NDPK) is a multifunctional protein that is involved in cell proliferation, development, as well as differentiation in eukaryotes. Aside from its basic enzymatic role involving phosphor-transfer as well as regeneration of nucleoside triphosphates, NDP kinase 2 is a component of the H<sub>2</sub>O<sub>2</sub>-activated MAPK signaling pathway in plants and its upregulation alters cellular redox conditions. The expression of NDPK2 is induced by H<sub>2</sub>O<sub>2</sub>, and knockout of NDPK2 results in increased ROS accumulation and stress sensitivity. On the other hand, upregulation of NDPK2 results in a decrease in H<sub>2</sub>O<sub>2</sub> levels and sensitivity to stress [71]. Catalase, peroxidase 2, and NDPK were downregulated during ripening (Fig 9A), whereas class III peroxidase 122 was upregulated by 2.76-fold

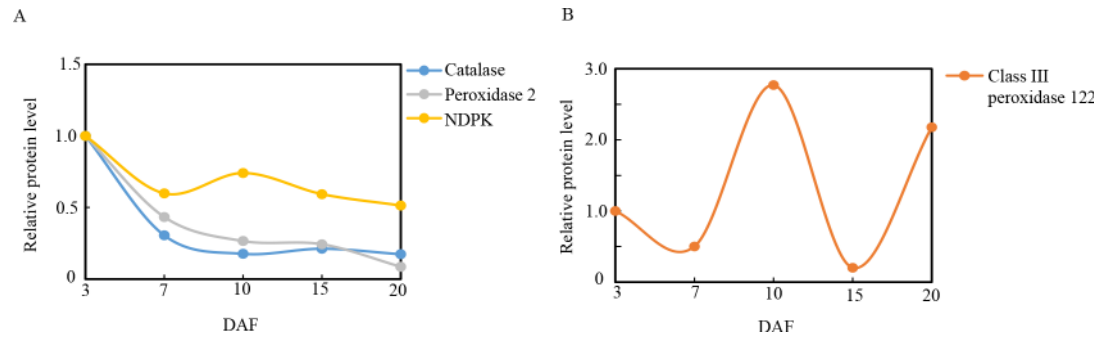


**Fig 9. Relative expression patterns of redox homeostasis proteins during grain development.** The expression level was established in relation to 3 days after flowering (DAF) (vertical axis) at various developmental stages (horizontal axis, DAF).

doi:10.1371/journal.pone.0159238.g009

in DAF10, sharply decreased in DAF15, and then upregulated by 2.18-fold at DAF20 (Fig 9B). The increase in class III peroxidase 122 activity directly correlated with protein abundance in proanthocyanidin-deficient *A. thaliana* seeds [72], and the increase in class III peroxidase 122 in DAF10 is correlated with changes in ACN levels. The pattern of antioxidant enzyme expression in grain development demonstrates that when the levels of catalase and peroxidase 2 activity decrease, class III peroxidase 122 (PODs) activity takes over to maintain redox homeostasis.

### Proteins involved in C-metabolism

Carbohydrates, or sugars, play a major role in plant growth. Recent studies have shown the stimulatory effects of sugars on the synthesis of ACNs in various organs of numerous plant species [73]. Previous investigations have proven that ACN biosynthesis occurs in plants that are germinated or grown on a sugar-containing medium [74–76]. In particular, the *CHS* gene of petunia (*Petunia hybrida*) petals in transgenic *Arabidopsis* leaves is activated by sugars [77], and petunia corollas that are cultured *in vitro* in the absence of sucrose (Suc) do not develop any pigmentation [78]. Tsukaya and Ohtoreported that *Arabidopsis* cultured on a Suc-containing medium produced high amounts of ACNs [77, 79]. Therefore, sugar content may play an essential role in ACN accumulation. In the present study, proteins involved in sugar metabolism included beta-galactosidase ( $\beta$ -GAL), sucrose synthase 4 (SUS4), pullulanase (pu1A), and starch-branching enzyme I (SBE I).

Grain development pertains to the synthesis and accumulation of starch in endosperm cells. Sucrose is continuously cleaved into UDP-glucose and utilized in starch synthesis. Starch biosynthesis is initiated using a substrate of ADP-glucose (ADP-Glu), which is formed by AGPase. ADP-Glu is transported into the cytoplasm via an ADP-glucose brittle-1 transporter. Various classes of sucrose synthase (SS) are recruited in order to lengthen the glucan chain, including SS 1–4 and granule-bound starch synthase, whereas starch-branching enzymes (SBEs) are involved in the formation of alpha-1,6-glucoside, and starch-debranching enzymes (DBEs) hydrolyze  $\alpha$ -(1,6) linkages of a polyglucan [80]. Three enzymes associated with sugar synthesis were detected in the present study, including SS4, SBE1, and Pullulanase [81]. All of these enzymes achieved the highest levels of expression at 10 DAF (Fig 10A). This is in agreement with the observed changes in ACN content. The  $\beta$ -GAL enzyme is an O-glycosyl hydrolase that hydrolyzes the glycosidic bond between 2 or more carbohydrates or between a carbohydrate and a non-carbohydrate moiety [82]. The present study demonstrated that  $\beta$ -GAL has a higher expression level at 3 DAF, but is dramatically downregulated at 10 DAF (Fig 10B), which could contribute to glucose accumulation and improve sucrose content during grain

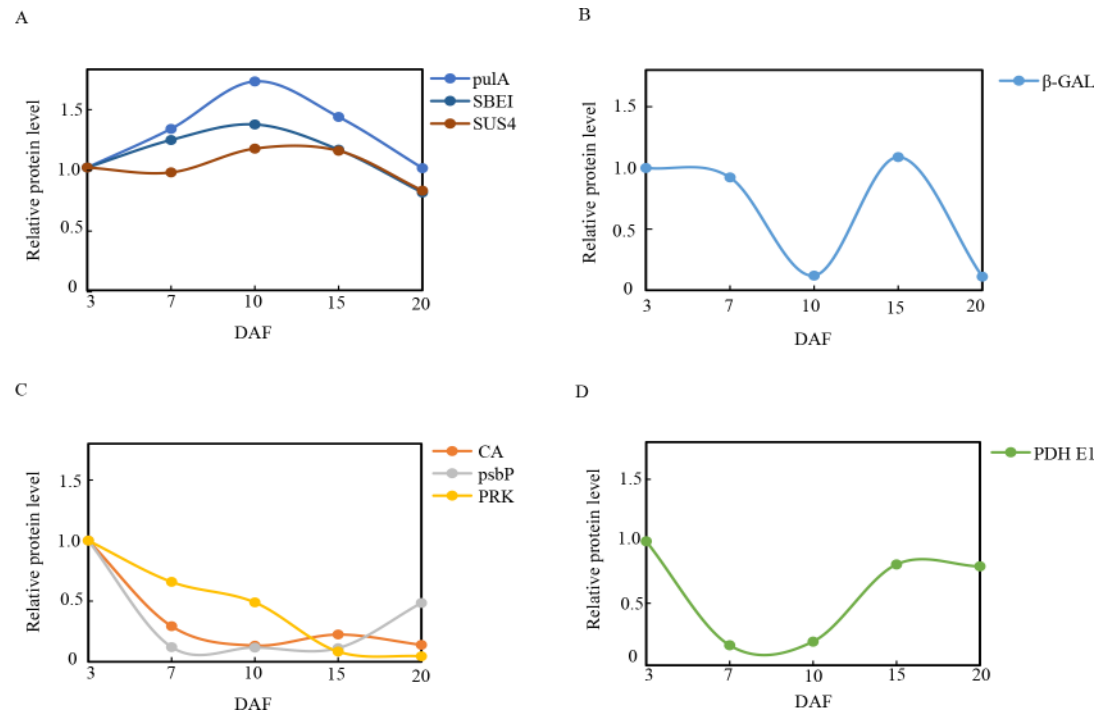


**Fig 10. Relative expression patterns of C-metabolism proteins during grain development.** The expression level was established in relation to 3 days after flowering (DAF) (vertical axis) at various developmental stages (horizontal axis, DAF).

doi:10.1371/journal.pone.0159238.g010

development. This result is concordant with previous reports that indicate that the onset of sucrose accumulation was accompanied by a decrease in  $\beta$ -GAL activity [83].

During the early grain stage, photosynthesis generates the raw material, triosephosphate, for starch biosynthesis, which plays an essential role in the maintenance of endogenous  $O_2$  balance [84]. The results of the present study showed that carbonic anhydrase (CA), chloroplast 23-kDa polypeptide of photosystem II (psbP), and phosphoribulokinase (PRK), which are necessary for photosynthesis, were upregulated at 3 DAF, particularly during the early grain development stages (Fig 10C), which in turn promoted plant photosynthesis as well as grain filling. The decline in the expression of these 3 enzymes during the later state of filling was suggestive of a down regulation of photosynthesis (Fig 10C), which has also been reported in tomatoes [85], apricots [86], grapes [87, 88], and palm [89]. The down regulation of proteins related to photosynthesis is correlated to the reduction in pyruvate dehydrogenase E1 component (PDH E1). The PDH E1 component is a major enzyme that catalyzes oxidative decarboxylation of pyruvate to acetyl CoA, which serves as the entry point of carbohydrates directly into the Krebs cycle [90]. In the present study, PDH E1 was downregulated on DAF7 and 10 (Fig 10D). This may indicate that while the photosynthetic rate declined, the decrease in abundance of the PDH E1 component reduced sugar consumption, which might be a signal that induces the acceleration of ACN biosynthesis [73].

### Proteins involved in N-metabolism

Plant growth and development are controlled by the concerted activities of signaling pathways, which are triggered by different environmental conditions as well as developmental cues. Nutrient availability, particularly N, is one of the major factors that regulate plant metabolism



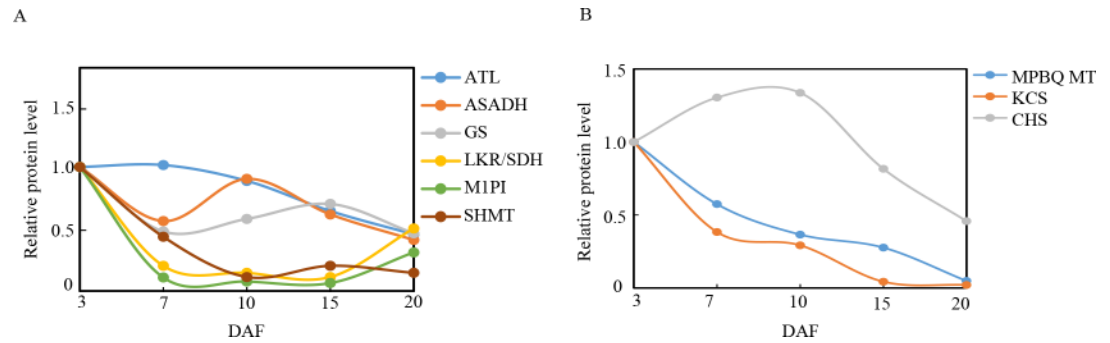


**Fig 11. Relative expression patterns of N-metabolism and functional proteins during grain development.** The expression level was established in relation to 3 days after flowering (DAF) (vertical axis) at various developmental stages (horizontal axis, DAF).

doi:10.1371/journal.pone.0159238.g011

and development [91]. N limitation induces ACN accumulation in plants, which in turn influences phenylpropanoid metabolic flux as well as switches ACN biosynthesis to lignin biosynthesis [92]. Proteins involved in N-metabolism that were identified in our study included glutamine synthetase (GS), alanine aminotransferase (ATL), aspartate-semialdehyde dehydrogenase (ASADH), lysine-ketoglutarate reductase/saccharopine dehydrogenase bifunctional enzyme (LKR/SDH), methylthioribose-1-phosphate isomerase (M1PI), and serine hydroxymethyltransferase (SHMT).

GS is triggers the first step of ammonium assimilation and transformation this into glutamine and glutamate, which are the major compounds of the amino acid biosynthetic pathway [93]. More than 95% of inorganic N in higher plants is assimilated and converted to glutamate and glutamine through the glutamine synthetase pathway, and then utilized in the generation of other amino acids during the catalysis of aspartate aminotransferase and alanine aminotransferase (ATL)[94]. The present study demonstrated that GS and ATL had a lower expression level at DAF 7 and 10 (Fig 11A), which was consistent with the findings of a proteomics study conducted by Zhang [95]. The decrease in GS and ATL during grain development may be attributable to N insufficiency and upregulated ACN synthesis and accumulation.

In plants, ASADH produces the branch point intermediate that occurs between the lysine and threonine/methionine pathways [96]. LKR/SDH is a bifunctional enzyme that catalyzes the first two steps of plant lysine catabolism, which controls the accumulation of different catabolic products of Lys[97]. M1PI functions in methionine salvage pathways in plants [98]. SHMT is a tetramer that induces the reversible conversion of serine and tetrahydrofolate (THF) into Gly and 5, 10-methylene THF [99]. The expression of 4 proteins (ASADH, LKR/SDH, M1PI, and SHMT) decreased during grain development (Fig 11A), which may contribute to insufficiency in N and induce ACN accumulation in black rice grains.

### Proteins involved in the flavonoid biosynthesis pathway

ACNs are generated by the phenylpropanoid pathway, which is initiated by the conversion of phenylalanine into cinnamic acid via phenylalanine ammonia lyase (PAL), and then diverges into various branches at *p*-coumaroyl CoA. One branch involves the flavonoid pathway, where in chalcone synthase (CHS) catalyzes the formation of the flavonoid skeleton, which is derived from *p*-coumaroyl CoA, and in turn leads to the synthesis of flavonols, cyanidins, and ACNs [92]. The present study showed that CHS was upregulated, peaking at DAF10, which corresponded to the middle of the grain development process. This protein was then downregulated at DAF20, when the development process was completed (Fig 11B). This result was correlated

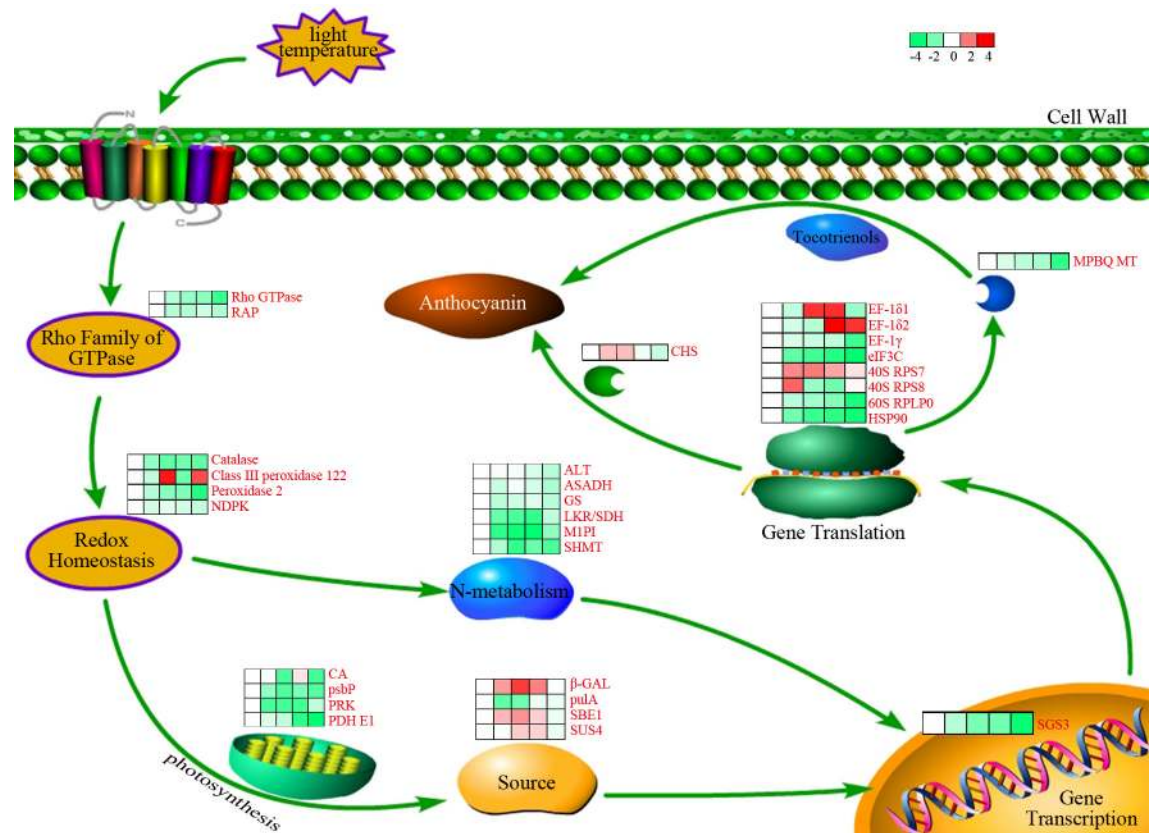


**Fig 12. Quantification of black rice grain proteins that are related to ACN biosynthesis.** RAP, Ras-related protein RIC2; NDPK, Nucleoside diphosphate kinase; CA, Carbonic anhydrase; psbP, Chloroplast 23-kDa polypeptide of photosystem II; PRK, Phosphoribulokinase; PDH E1, Pyruvate dehydrogenase E1 component subunit alpha; β-GAL, Beta-galactosidase; puA, Pullulanase; SBE1, Starch-branching enzyme I; SUS4, Sucrose synthase 4; ALT, Alanine aminotransferase; ASADH, Aspartate-semialdehyde dehydrogenase family protein; GS, Glutamine synthetase; LKR/SDH, Putative lysine-ketoglutarate reductase/saccharopine dehydrogenase bifunctional enzyme; M1PI, Methylthioribose-1-phosphate isomerase; SHMT, Serine hydroxymethyltransferase; SGS3, Protein SUPPRESSOR OF GENE SILENCING 3 homolog; MPBQ MT, 2-methyl-6-phytyl-1,4-hydroquinone methyltransferase 2; EF-1δ1, Elongation factor 1-delta 1; EF-1δ2, Elongation factor 1-delta 2; EF-1γ, Elongation factor 1-gamma; eIF3C, Eukaryotic translation initiation factor 3 subunit C; 40S RPS7, 40S ribosomal protein S7; 40S RPS8, 40S ribosomal protein S8; 60S RPLP0, 60S acidic ribosomal protein P0; HSP90, Hsp90 protein; CHS, Chalcone synthase 1. The protein levels of deregulated enzymes are indicated by colored squares that represent changes in expression (log<sub>2</sub> ratio) at various developmental stages in relation to the 3 DAF stage. In a sequence order (left to right), stages are presented from 3, 7, 10, 15, and 20 DAF.

doi:10.1371/journal.pone.0159238.g012

with the observed expression level of CHS in *P. dactylifera* [89], and the changing trends of ACN contents in the present study.

### Proteins involved in the tocopherol biosynthetic pathway

Tocotrienols pertain to the primary form of vitamin E present in seeds of majority of monocot plants, including cereals (e.g., rice and wheat) [100]. 2-Methyl-6-phytyl-1,4-hydroquinone methyltransferase 2 (MPBQ MT) is a major component enzyme that is involved in the key methylation step in tocopherol (vitamin E) synthesis, which mediates the conversion of 2-methyl-6-phytyl-1,4-hydroquinone into 2,3-dimethyl-6-phytyl-1,4-hydroquinone and 2-methyl-6-solanlyl-1,4-benzoquinone to plastoquinone. Recent studies on the tocopherol-deficient *vte1* mutants of *A. thaliana* indicated that the down regulation of tocopherol increases jasmonic acid levels in plants, whereas ACN biosynthesis in epidermal, vascular, and mesophyll cells are upregulated by

jasmonic acid [101, 102]. In the present study, MPBQ MT was increasingly downregulated from 3 to 20DAF (Fig 11B), which may have induced ACN biosynthesis by upregulating jasmonic acid levels.

## Proteins involved in fatty acid pathways

Very long-chain fatty acids (VLCFAs) are essential precursors of cuticular waxes as well as aliphatic suberins in plants. The condensation of C units into an acyl CoA via 3-ketoacyl CoA synthase (KCS) is the first committed step of VLCFA biosynthesis [103]. In the present study, KCS was downregulated during rice grain development (Fig 11B). The observed decrease in KCS was correlated with a reduction in fatty acid synthesis during grain development.

## Conclusions

In summary, we investigated the dynamic changes in protein expression levels during five sequential developmental stages that were associated with black rice grain filling, namely from 3 to 20 DAF. The results of the present study indicated that during plant development, proteins involved in both flavonoid and starch synthesis are upregulated, and proteins that were related to other categories and subcategories were downregulated. Importantly, the present study revealed that CHS is a key enzyme in the ACN biosynthetic pathway in black rice. In addition, we determined that a high sugar content and deficiency in N metabolism promoted ACN biosynthesis. Our results also showed that the coordination of various metabolic and cellular processes is related to ACN synthesis and accumulation during seed development. A simple model of pathways associated with ACN biosynthesis is presented in Fig 12. The results of the present study provide novel clues that facilitate in better understanding the metabolic network that is involved in ACN accumulation in developing seeds.

## Supporting Information

**S1 Table. Differentially expressed proteins in black rice grains at five developmental stages.** (XLSX)

## Acknowledgments

This work was supported by the National Key Technology R&D Program (2013BAD01B05) and the Science and Technology Innovation Platform Development Program of Fujian Agriculture and Forestry University (PTJH13001, PTJH12015). We gratefully acknowledge Shanghai Omicspace Biotechnology Co. Ltd. for technical assistance with the peptide/protein identification.

## Author Contributions

Conceived and designed the experiments: JZ LC. Performed the experiments: LC YH. Analyzed the data: MX. Contributed reagents/materials/analysis tools: ZC. Wrote the paper: DZ JZ.

## References

1. Wang E, Wang J, Zhu X, Hao W, Wang L, Li Q, et al. Control of rice grain-filling and yield by a gene with a potential signature of domestication. *Nature genetics*. 2008; 40(11):1370–4. Epub 2008/09/30. doi: [10.1038/ng.220](https://doi.org/10.1038/ng.220) PMID: [18820698](https://pubmed.ncbi.nlm.nih.gov/18820698/).
2. Ichikawa H, Ichiyangi T, Xu B, Yoshii Y, Nakajima M, Konishi T. Antioxidant Activity of Anthocyanin Extract from Purple Black Rice. *Journal of medicinal food*. 2001; 4(4):211–8. Epub 2003/03/18. doi: [10.1089/10966200152744481](https://doi.org/10.1089/10966200152744481) PMID: [12639403](https://pubmed.ncbi.nlm.nih.gov/12639403/).

3. Kim CK, Cho MA, Choi YH, Kim JA, Kim YH, Kim YK, et al. Identification and characterization of seed-specific transcription factors regulating anthocyanin biosynthesis in black rice. *Journal of applied genetics*. 2011; 52(2):161–9. Epub 2011/02/03. doi: [10.1007/s13353-011-0027-3](https://doi.org/10.1007/s13353-011-0027-3) PMID: [21286901](https://pubmed.ncbi.nlm.nih.gov/21286901/); PubMed Central PMCID: [PMC3088801](https://pubmed.ncbi.nlm.nih.gov/PMC3088801/).
4. Ryu SN, Park SZ, Ho CT. High performance liquid chromatographic determination of anthocyanin pigments in some varieties of black rice. *Journal of food and Drug Analysis*. 1998; 6(4):729–36.
5. Wang Q, Han P, Zhang M, Xia M, Zhu H, Ma J, et al. Supplementation of black rice pigment fraction improves antioxidant and anti-inflammatory status in patients with coronary heart disease. *Asia Pacific journal of clinical nutrition*. 2007; 16 Suppl 1:295–301. Epub 2007/03/30. PMID: [17392122](https://pubmed.ncbi.nlm.nih.gov/17392122/).
6. Wu X, Beecher GR, Holden JM, Haytowitz DB, Gebhardt SE, Prior RL. Concentrations of anthocyanins in common foods in the United States and estimation of normal consumption. *Journal of agricultural and food chemistry*. 2006; 54(11):4069–75. Epub 2006/05/25. doi: [10.1021/jf060300l](https://doi.org/10.1021/jf060300l) PMID: [16719536](https://pubmed.ncbi.nlm.nih.gov/16719536/).
7. Hiemori M, Koh E, Mitchell AE. Influence of cooking on anthocyanins in black rice (*Oryza sativa* L. japonica var. SBR). *Journal of agricultural and food chemistry*. 2009; 57(5):1908–14. Epub 2009/03/05. doi: [10.1021/jf803153z](https://doi.org/10.1021/jf803153z) PMID: [19256557](https://pubmed.ncbi.nlm.nih.gov/19256557/).
8. Philpott M, Gould KS, Lim C, Ferguson LR. In situ and in vitro antioxidant activity of sweetpotato anthocyanins. *Journal of agricultural and food chemistry*. 2004; 52(6):1511–3. Epub 2004/03/20. doi: [10.1021/jf034593j](https://doi.org/10.1021/jf034593j) PMID: [15030203](https://pubmed.ncbi.nlm.nih.gov/15030203/).
9. Nam SH, Choi SP, Kang MY, Koh HJ, Kozukue N, Friedman M. Antioxidative activities of bran extracts from twenty one pigmented rice cultivars. *Food Chemistry*. 2006; 94(4):613–20.
10. Renaud S, de Lorgeril M. Wine, alcohol, platelets, and the French paradox for coronary heart disease. *Lancet (London, England)*. 1992; 339(8808):1523–6. Epub 1992/06/20. PMID: [1351198](https://pubmed.ncbi.nlm.nih.gov/1351198/).
11. Joseph JA, Shukitt-Hale B, Denisova NA, Bielinski D, Martin A, McEwen JJ, et al. Reversals of age-related declines in neuronal signal transduction, cognitive, and motor behavioral deficits with blueberry, spinach, or strawberry dietary supplementation. *The Journal of neuroscience: the official journal of the Society for Neuroscience*. 1999; 19(18):8114–21. Epub 1999/09/10. PMID: [10479711](https://pubmed.ncbi.nlm.nih.gov/10479711/).
12. Seeram NP, Adams LS, Hardy ML, Heber D. Total cranberry extract versus its phytochemical constituents: antiproliferative and synergistic effects against human tumor cell lines. *Journal of agricultural and food chemistry*. 2004; 52(9):2512–7. Epub 2004/04/29. doi: [10.1021/jf0352778](https://doi.org/10.1021/jf0352778) PMID: [15113149](https://pubmed.ncbi.nlm.nih.gov/15113149/).
13. Hou DX, Fujii M, Terahara N, Yoshimoto M. Molecular Mechanisms Behind the Chemopreventive Effects of Anthocyanidins. *Journal of biomedicine & biotechnology*. 2004; 2004(5):321–5. Epub 2004/12/04. doi: [10.1155/s110724304403040](https://doi.org/10.1155/s110724304403040) PMID: [15577196](https://pubmed.ncbi.nlm.nih.gov/15577196/); PubMed Central PMCID: [PMC308887](https://pubmed.ncbi.nlm.nih.gov/PMC308887/).
14. Xia X, Ling W, Ma J, Xia M, Hou M, Wang Q, et al. An anthocyanin-rich extract from black rice enhances atherosclerotic plaque stabilization in apolipoprotein E-deficient mice. *The Journal of nutrition*. 2006; 136(8):2220–5. Epub 2006/07/22. PMID: [16857844](https://pubmed.ncbi.nlm.nih.gov/16857844/).
15. Kwon SH, Ahn IS, Kim SO, Kong CS, Chung HY, Do MS, et al. Anti-obesity and hypolipidemic effects of black soybean anthocyanins. *Journal of medicinal food*. 2007; 10(3):552–6. Epub 2007/09/25. doi: [10.1089/jmf.2006.147](https://doi.org/10.1089/jmf.2006.147) PMID: [17887951](https://pubmed.ncbi.nlm.nih.gov/17887951/).
16. Guo H, Ling W, Wang Q, Liu C, Hu Y, Xia M, et al. Effect of anthocyanin-rich extract from black rice (*Oryza sativa* L. indica) on hyperlipidemia and insulin resistance in fructose-fed rats. *Plant foods for human nutrition (Dordrecht, Netherlands)*. 2007; 62(1):1–6. Epub 2006/12/26. doi: [10.1007/s11130-006-0031-7](https://doi.org/10.1007/s11130-006-0031-7) PMID: [17187297](https://pubmed.ncbi.nlm.nih.gov/17187297/).
17. Sasaki R, Nishimura N, Hoshino H, Isa Y, Kadowaki M, Ichi T, et al. Cyanidin 3-glucoside ameliorates hyperglycemia and insulin sensitivity due to downregulation of retinol binding protein 4 expression in diabetic mice. *Biochemical pharmacology*. 2007; 74(11):1619–27. Epub 2007/09/18. doi: [10.1016/j.bcp.2007.08.008](https://doi.org/10.1016/j.bcp.2007.08.008) PMID: [17869225](https://pubmed.ncbi.nlm.nih.gov/17869225/).
18. Matsumoto H, Nakamura Y, Tachibanaki S, Kawamura S, Hirayama M. Stimulatory effect of cyanidin 3-glycosides on the regeneration of rhodopsin. *Journal of agricultural and food chemistry*. 2003; 51(12):3560–3. Epub 2003/05/29. doi: [10.1021/jf034132y](https://doi.org/10.1021/jf034132y) PMID: [12769524](https://pubmed.ncbi.nlm.nih.gov/12769524/).
19. Tsuda T, Horio F, Uchida K, Aoki H, Osawa T. Dietary cyanidin 3-O-beta-D-glucoside-rich purple corn color prevents obesity and ameliorates hyperglycemia in mice. *The Journal of nutrition*. 2003; 133(7):2125–30. Epub 2003/07/04. PMID: [12840166](https://pubmed.ncbi.nlm.nih.gov/12840166/).
20. Wilmouth RC, Turnbull JJ, Welford RW, Clifton IJ, Prescott AG, Schofield CJ. Structure and mechanism of anthocyanidin synthase from *Arabidopsis thaliana*. *Structure (London, England: 1993)*. 2002; 10(1):93–103. Epub 2002/02/14. PMID: [11796114](https://pubmed.ncbi.nlm.nih.gov/11796114/).
21. Christie PJ, Alfenito MR, Walbot V. Impact of low-temperature stress on general phenylpropanoid and anthocyanin pathways: enhancement of transcript abundance and anthocyanin pigmentation in maize seedlings. *Planta*. 1994; 194(4):541–9.

22. Mori K, Sugaya S, Gemma H. Decreased anthocyanin biosynthesis in grape berries grown under elevated night temperature condition. *Scientia Horticulturae*. 2005; 105(3):319–30.
23. Lo Piero AR, Puglisi I, Rapisarda P, Petrone G. Anthocyanins accumulation and related gene expression in red orange fruit induced by low temperature storage. *Journal of agricultural and food chemistry*. 2005; 53(23):9083–8. Epub 2005/11/10. doi: [10.1021/jf051609s](https://doi.org/10.1021/jf051609s) PMID: [16277406](https://pubmed.ncbi.nlm.nih.gov/16277406/).
24. Ubi BE, Honda C, Bessho H, Kondo S, Wada M, Kobayashi S, et al. Expression analysis of anthocyanin biosynthetic genes in apple skin: effect of UV-B and temperature. *Plant Science*. 2006; 170(3):571–8.
25. He F, Pan QH, Shi Y, Duan CQ. Biosynthesis and genetic regulation of proanthocyanidins in plants. *Molecules (Basel, Switzerland)*. 2008; 13(10):2674–703. Epub 2008/10/31. doi: [10.3390/molecules13102674](https://doi.org/10.3390/molecules13102674) PMID: [18971863](https://pubmed.ncbi.nlm.nih.gov/18971863/).
26. Zhang Y, Butelli E, Martin C. Engineering anthocyanin biosynthesis in plants. *Current opinion in plant biology*. 2014; 19:81–90. Epub 2014/06/08. doi: [10.1016/j.pbi.2014.05.011](https://doi.org/10.1016/j.pbi.2014.05.011) PMID: [24907528](https://pubmed.ncbi.nlm.nih.gov/24907528/).
27. Holton TA, Cornish EC. Genetics and Biochemistry of Anthocyanin Biosynthesis. *The Plant cell*. 1995; 7(7):1071–83. Epub 1995/07/01. doi: [10.1105/tpc.7.7.1071](https://doi.org/10.1105/tpc.7.7.1071) PMID: [12242398](https://pubmed.ncbi.nlm.nih.gov/12242398/); PubMed Central PMCID: PMC160913.
28. Lepiniec L, Debeaujon I, Routaboul JM, Baudry A, Pourcel L, Nesi N, et al. Genetics and biochemistry of seed flavonoids. *Annual review of plant biology*. 2006; 57:405–30. Epub 2006/05/04. doi: [10.1146/annurev.arplant.57.032905.105252](https://doi.org/10.1146/annurev.arplant.57.032905.105252) PMID: [16669768](https://pubmed.ncbi.nlm.nih.gov/16669768/).
29. Kim BG, Kim JH, Min SY, Shin K-H, Kim JH, Kim HY, et al. Anthocyanin content in rice is related to expression levels of anthocyanin biosynthetic genes. *Journal of Plant Biology*. 2007; 50(2):156–60.
30. Tian Q, Giusti MM, Stoner GD, Schwartz SJ. Screening for anthocyanins using high-performance liquid chromatography coupled to electrospray ionization tandem mass spectrometry with precursor-ion analysis, product-ion analysis, common-neutral-loss analysis, and selected reaction monitoring. *Journal of chromatography A*. 2005; 1091(1–2):72–82. Epub 2006/01/06. PMID: [16395794](https://pubmed.ncbi.nlm.nih.gov/16395794/).
31. Hu C, Zawistowski J, Ling W, Kitts DD. Black rice (*Oryza sativa* L. indica) pigmented fraction suppresses both reactive oxygen species and nitric oxide in chemical and biological model systems. *Journal of agricultural and food chemistry*. 2003; 51(18):5271–7. Epub 2003/08/21. doi: [10.1021/jf034466n](https://doi.org/10.1021/jf034466n) PMID: [12926869](https://pubmed.ncbi.nlm.nih.gov/12926869/).
32. Abdel-Aal el SM, Young JC, Rabalski I. Anthocyanin composition in black, blue, pink, purple, and red cereal grains. *Journal of agricultural and food chemistry*. 2006; 54(13):4696–704. Epub 2006/06/22. doi: [10.1021/jf0606609](https://doi.org/10.1021/jf0606609) PMID: [16787017](https://pubmed.ncbi.nlm.nih.gov/16787017/).
33. Ding M, Feng R, Wang SY, Bowman L, Lu Y, Qian Y, et al. Cyanidin-3-glucoside, a natural product derived from blackberry, exhibits chemopreventive and chemotherapeutic activity. *The Journal of biological chemistry*. 2006; 281(25):17359–68. Epub 2006/04/19. doi: [10.1074/jbc.M600861200](https://doi.org/10.1074/jbc.M600861200) PMID: [16618699](https://pubmed.ncbi.nlm.nih.gov/16618699/).
34. Kim C-K, Cho M-A, Choi Y-H, Kim J-A, Kim Y-H, Kim Y-K, et al. Identification and characterization of seed-specific transcription factors regulating anthocyanin biosynthesis in black rice. *Journal of applied genetics*. 2011; 52(2):161–9. doi: [10.1007/s13353-011-0027-3](https://doi.org/10.1007/s13353-011-0027-3) PMID: [21286901](https://pubmed.ncbi.nlm.nih.gov/21286901/)
35. Anderson NL, Anderson NG. Proteome and proteomics: new technologies, new concepts, and new words. *Electrophoresis*. 1998; 19(11):1853–61. Epub 1998/09/18. doi: [10.1002/elps.1150191103](https://doi.org/10.1002/elps.1150191103) PMID: [9740045](https://pubmed.ncbi.nlm.nih.gov/9740045/).
36. Xu SB, Li T, Deng ZY, Chong K, Xue Y, Wang T. Dynamic proteomic analysis reveals a switch between central carbon metabolism and alcoholic fermentation in rice filling grains. *Plant physiology*. 2008; 148(2):908–25. Epub 2008/08/30. doi: [10.1104/pp.108.125633](https://doi.org/10.1104/pp.108.125633) PMID: [18753281](https://pubmed.ncbi.nlm.nih.gov/18753281/); PubMed Central PMCID: PMC160913.
37. Xu SB, Yu HT, Yan LF, Wang T. Integrated proteomic and cytological study of rice endosperms at the storage phase. *Journal of proteome research*. 2010; 9(10):4906–18. Epub 2010/08/18. doi: [10.1021/pr900954p](https://doi.org/10.1021/pr900954p) PMID: [20712379](https://pubmed.ncbi.nlm.nih.gov/20712379/).
38. Lin SK, Chang MC, Tsai YG, Lur HS. Proteomic analysis of the expression of proteins related to rice quality during caryopsis development and the effect of high temperature on expression. *Proteomics*. 2005; 5(8):2140–56. Epub 2005/04/27. doi: [10.1002/pmic.200401105](https://doi.org/10.1002/pmic.200401105) PMID: [15852341](https://pubmed.ncbi.nlm.nih.gov/15852341/).
39. Chu P, Yan GX, Yang Q, Zhai LN, Zhang C, Zhang FQ, et al. iTRAQ-based quantitative proteomics analysis of *Brassica napus* leaves reveals pathways associated with chlorophyll deficiency. *Journal of proteomics*. 2015; 113:244–59. Epub 2014/10/16. doi: [10.1016/j.jprot.2014.10.005](https://doi.org/10.1016/j.jprot.2014.10.005) PMID: [25317966](https://pubmed.ncbi.nlm.nih.gov/25317966/).
40. Vertommen A, Panis B, Swennen R, Carpentier SC. Challenges and solutions for the identification of membrane proteins in non-model plants. *Journal of proteomics*. 2011; 74(8):1165–81. Epub 2011/03/01. doi: [10.1016/j.jprot.2011.02.016](https://doi.org/10.1016/j.jprot.2011.02.016) PMID: [21354347](https://pubmed.ncbi.nlm.nih.gov/21354347/).

41. Nunn BL, Aker JR, Shaffer SA, Tsai S, Strzepek RF, Boyd PW, et al. Deciphering diatom biochemical pathways via whole-cell proteomics. *Aquatic microbial ecology: international journal*. 2009; 55(3):241–53. Epub 2009/10/16. doi: [10.3354/ame01284](https://doi.org/10.3354/ame01284) PMID: [19829762](https://pubmed.ncbi.nlm.nih.gov/19829762/); PubMed Central PMCID: [PMCpmc2761042](https://pubmed.ncbi.nlm.nih.gov/PMC/PMCpmc2761042/).
42. Ryu S, Gallis B, Goo YA, Shaffer SA, Radulovic D, Goodlett DR. Comparison of a label-free quantitative proteomic method based on peptide ion current area to the isotope coded affinity tag method. *Cancer informatics*. 2008; 6:243–55. Epub 2008/01/01. PMID: [19259412](https://pubmed.ncbi.nlm.nih.gov/19259412/); PubMed Central PMCID: [PMCpmc2623286](https://pubmed.ncbi.nlm.nih.gov/PMC/PMCpmc2623286/).
43. Chen J, Ryu S, Gharib SA, Goodlett DR, Schnapp LM. Exploration of the normal human bronchoalveolar lavage fluid proteome. *Proteomics Clinical applications*. 2008; 2(4):585–95. Epub 2008/04/01. doi: [10.1002/prca.200780006](https://doi.org/10.1002/prca.200780006) PMID: [21136857](https://pubmed.ncbi.nlm.nih.gov/21136857/); PubMed Central PMCID: [PMCpmc4432467](https://pubmed.ncbi.nlm.nih.gov/PMC/PMCpmc4432467/).
44. Du C, Liang JR, Chen DD, Xu B, Zhuo WH, Gao YH, et al. iTRAQ-based proteomic analysis of the metabolism mechanism associated with silicon response in the marine diatom *Thalassiosira pseudonana*. *Journal of proteome research*. 2014; 13(2):720–34. Epub 2014/01/01. doi: [10.1021/pr400803w](https://doi.org/10.1021/pr400803w) PMID: [24372006](https://pubmed.ncbi.nlm.nih.gov/24372006/).
45. Ma C, Zhou J, Chen G, Bian Y, Lv D, Li X, et al. iTRAQ-based quantitative proteome and phosphoprotein characterization reveals the central metabolism changes involved in wheat grain development. *BMC genomics*. 2014; 15:1029. Epub 2014/11/28. doi: [10.1186/1471-2164-15-1029](https://doi.org/10.1186/1471-2164-15-1029) PMID: [25427527](https://pubmed.ncbi.nlm.nih.gov/25427527/); PubMed Central PMCID: [PMCpmc4301063](https://pubmed.ncbi.nlm.nih.gov/PMC/PMCpmc4301063/).
46. Kambiranda D, Katam R, Basha SM, Siebert S. iTRAQ-based quantitative proteomics of developing and ripening muscadine grape berry. *Journal of proteome research*. 2014; 13(2):555–69. Epub 2013/11/21. doi: [10.1021/pr400731p](https://doi.org/10.1021/pr400731p) PMID: [24251720](https://pubmed.ncbi.nlm.nih.gov/24251720/); PubMed Central PMCID: [PMCpmc3970428](https://pubmed.ncbi.nlm.nih.gov/PMC/PMCpmc3970428/).
47. Martinez-Esteso MJ, Vilella-Anton MT, Pedreno MA, Valero ML, Bru-Martinez R. iTRAQ-based protein profiling provides insights into the central metabolism changes driving grape berry development and ripening. *BMC plant biology*. 2013; 13:167. Epub 2013/10/25. doi: [10.1186/1471-2229-13-167](https://doi.org/10.1186/1471-2229-13-167) PMID: [24152288](https://pubmed.ncbi.nlm.nih.gov/24152288/); PubMed Central PMCID: [PMCpmc4016569](https://pubmed.ncbi.nlm.nih.gov/PMC/PMCpmc4016569/).
48. Lucker J, Laszczak M, Smith D, Lund ST. Generation of a predicted protein database from EST data and application to iTRAQ analyses in grape (*Vitis vinifera* cv. Cabernet Sauvignon) berries at ripening initiation. *BMC genomics*. 2009; 10:50. Epub 2009/01/28. doi: [10.1186/1471-2164-10-50](https://doi.org/10.1186/1471-2164-10-50) PMID: [19171055](https://pubmed.ncbi.nlm.nih.gov/19171055/); PubMed Central PMCID: [PMCpmc2637896](https://pubmed.ncbi.nlm.nih.gov/PMC/PMCpmc2637896/).
49. Dong M, Gu J, Zhang L, Chen P, Liu T, Deng J, et al. Comparative proteomics analysis of superior and inferior spikelets in hybrid rice during grain filling and response of inferior spikelets to drought stress using isobaric tags for relative and absolute quantification. *Journal of proteomics*. 2014; 109:382–99. Epub 2014/07/25. doi: [10.1016/j.jprot.2014.07.001](https://doi.org/10.1016/j.jprot.2014.07.001) PMID: [25058577](https://pubmed.ncbi.nlm.nih.gov/25058577/).
50. Ishimaru T, Matsuda T, Ohsugi R, Yamagishi T. Morphological development of rice caryopses located at the different positions in a panicle from early to middle stage of grain filling. *Functional Plant Biology*. 2003; 30(11):1139–49.
51. Abdel-Aal E-S, Hucl P. A rapid method for quantifying total anthocyanins in blue aleurone and purple pericarp wheats. *Cereal chemistry*. 1999; 76(3):350–4.
52. Dai S, Chen T, Chong K, Xue Y, Liu S, Wang T. Proteomics identification of differentially expressed proteins associated with pollen germination and tube growth reveals characteristics of germinated *Oryza sativa* pollen. *Molecular & cellular proteomics: MCP*. 2007; 6(2):207–30. Epub 2006/11/30. doi: [10.1074/mcp.M600146-MCP200](https://doi.org/10.1074/mcp.M600146-MCP200) PMID: [17132620](https://pubmed.ncbi.nlm.nih.gov/17132620/).
53. Wisniewski JR, Zougman A, Nagaraj N, Mann M. Universal sample preparation method for proteome analysis. *Nature methods*. 2009; 6(5):359–62. Epub 2009/04/21. doi: [10.1038/nmeth.1322](https://doi.org/10.1038/nmeth.1322) PMID: [19377485](https://pubmed.ncbi.nlm.nih.gov/19377485/).
54. Cox J, Mann M. MaxQuant enables high peptide identification rates, individualized p.p.b.-range mass accuracies and proteome-wide protein quantification. *Nature biotechnology*. 2008; 26(12):1367–72. Epub 2008/11/26. doi: [10.1038/nbt.1511](https://doi.org/10.1038/nbt.1511) PMID: [19029910](https://pubmed.ncbi.nlm.nih.gov/19029910/).
55. Chong PM, Lynch T, McCorrister S, Kibsey P, Miller M, Gravel D, et al. Proteomic analysis of a NAP1 *Clostridium difficile* clinical isolate resistant to metronidazole. *PloS one*. 2014; 9(1):e82622. Epub 2014/01/09. doi: [10.1371/journal.pone.0082622](https://doi.org/10.1371/journal.pone.0082622) PMID: [24400070](https://pubmed.ncbi.nlm.nih.gov/24400070/); PubMed Central PMCID: [PMCpmc3882210](https://pubmed.ncbi.nlm.nih.gov/PMC/PMCpmc3882210/).
56. Conesa A, Gotz S, Garcia-Gomez JM, Terol J, Talon M, Robles M. Blast2GO: a universal tool for annotation, visualization and analysis in functional genomics research. *Bioinformatics (Oxford, England)*. 2005; 21(18):3674–6. Epub 2005/08/06. doi: [10.1093/bioinformatics/bti610](https://doi.org/10.1093/bioinformatics/bti610) PMID: [16081474](https://pubmed.ncbi.nlm.nih.gov/16081474/).
57. Tatusov RL, Koonin EV, Lipman DJ. A genomic perspective on protein families. *Science (New York, NY)*. 1997; 278(5338):631–7. Epub 1997/10/24. PMID: [9381173](https://pubmed.ncbi.nlm.nih.gov/9381173/).

58. Oike Y, Tabata M. Angiopoietin-like proteins—potential therapeutic targets for metabolic syndrome and cardiovascular disease. *Circulation journal: official journal of the Japanese Circulation Society*. 2009; 73(12):2192–7. Epub 2009/10/31. PMID: [19875897](#).
59. Pfaffl MW. A new mathematical model for relative quantification in real-time RT-PCR. *Nucleic acids research*. 2001; 29(9):e45. Epub 2001/05/09. PMID: [11328886](#); PubMed Central PMCID: PMC55695.
60. Shao Y, Xu F, Sun X, Bao J, Beta T. Phenolic acids, anthocyanins, and antioxidant capacity in rice (*Oryza sativa* L.) grains at four stages of development after flowering. *Food Chem*. 2014; 143:90–6. Epub 2013/09/24. doi: [10.1016/j.foodchem.2013.07.042](#) PMID: [24054217](#).
61. Sompong R, Siebenhandl-Ehn S, Linsberger-Martin G, Berghofer E. Physicochemical and antioxidative properties of red and black rice varieties from Thailand, China and Sri Lanka. *Food Chemistry*. 2011; 124(1):132–40.
62. Xu SB, Yu HT, Yan LF, Wang T. Integrated proteomic and cytological study of rice endosperms at the storage phase. *Journal of proteome research*. 2010; 9(10):4906–18. doi: [10.1021/pr900954p](#) PMID: [20712379](#)
63. He D, Han C, Yao J, Shen S, Yang P. Constructing the metabolic and regulatory pathways in germinating rice seeds through proteomic approach. *Proteomics*. 2011; 11(13):2693–713. Epub 2011/06/02. doi: [10.1002/pmic.201000598](#) PMID: [21630451](#).
64. Lin Y, Wang Y, Zhu J, Yang Z. Localization of a Rho GTPase implies a role in tip growth and movement of the generative cell in pollen tubes. *The Plant Cell*. 1996; 8(2):293–303. PMID: [12239385](#)
65. Shan X, Zhang Y, Peng W, Wang Z, Xie D. Molecular mechanism for jasmonate-induction of anthocyanin accumulation in *Arabidopsis*. *Journal of experimental botany*. 2009; 60(13):3849–60. doi: [10.1093/jxb/erp223](#) PMID: [19596700](#)
66. Xia C, Wang YJ, Li WQ, Chen YR, Deng Y, Zhang XQ, et al. The *Arabidopsis* eukaryotic translation initiation factor 3, subunit F (AtelF3f), is required for pollen germination and embryogenesis. *The Plant Journal*. 2010; 63(2):189–202. doi: [10.1111/j.1365-3113X.2010.04237.x](#) PMID: [20444226](#)
67. Di Carli M, Zamboni A, Pe ME, Pezzotti M, Lilley KS, Benvenuto E, et al. Two-dimensional differential in gel electrophoresis (2D-DIGE) analysis of grape berry proteome during postharvest withering. *Journal of proteome research*. 2010; 10(2):429–46. doi: [10.1021/pr1005313](#) PMID: [20945943](#)
68. Voinnet O, Pinto YM, Baulcombe DC. Suppression of gene silencing: a general strategy used by diverse DNA and RNA viruses of plants. *Proceedings of the National Academy of Sciences*. 1999; 96(24):14147–52.
69. Foyer CH, Noctor G. Redox homeostasis and antioxidant signaling: a metabolic interface between stress perception and physiological responses. *The Plant Cell*. 2005; 17(7):1866–75. PMID: [15987996](#)
70. Page M, Sultana N, Paszkiewicz K, Florance H, Smirnoff N. The influence of ascorbate on anthocyanin accumulation during high light acclimation in *Arabidopsis thaliana*: further evidence for redox control of anthocyanin synthesis. *Plant, cell & environment*. 2012; 35(2):388–404.
71. Moon H, Lee B, Choi G, Shin D, Prasad DT, Lee O, et al. NDP kinase 2 interacts with two oxidative stress-activated MAPKs to regulate cellular redox state and enhances multiple stress tolerance in transgenic plants. *Proceedings of the National Academy of Sciences*. 2003; 100(1):358–63.
72. Jia L, Xu W, Li W, Ye N, Liu R, Shi L, et al. Class III peroxidases are activated in proanthocyanidin-deficient *Arabidopsis thaliana* seeds. *Annals of botany*. 2013; 111(5):839–47. doi: [10.1093/aob/mct045](#) PMID: [23448691](#)
73. Solfanelli C, Poggi A, Loreti E, Alpi A, Perata P. Sucrose-specific induction of the anthocyanin biosynthetic pathway in *Arabidopsis*. *Plant physiology*. 2006; 140(2):637–46. PMID: [16384906](#)
74. Baier M, Hemmann G, Holman R, Corke F, Card R, Smith C, et al. Characterization of mutants in *Arabidopsis* showing increased sugar-specific gene expression, growth, and developmental responses. *Plant Physiology*. 2004; 134(1):81–91. PMID: [14684841](#)
75. Németh K, Salchert K, Putnoky P, Bhalerao R, Koncz-Kálmán Z, Stankovic-Stangeland B, et al. Pleiotropic control of glucose and hormone responses by PRL1, a nuclear WD protein, in *Arabidopsis*. *Genes & development*. 1998; 12(19):3059–73.
76. Mita S, Hirano H, Nakamura K. Negative Regulation in the Expression of a Sugar-Inducible Gene in *Arabidopsis thaliana* (A Recessive Mutation Causing Enhanced Expression of a Gene for [beta]-Amylase). *Plant physiology*. 1997; 114(2):575–82. PMID: [9193090](#)
77. Tsukaya H, Ohshima T, Naito S, Chino M, Komeda Y. Sugar-dependent expression of the CHS-A gene for chalcone synthase from petunia in transgenic *Arabidopsis*. *Plant Physiology*. 1991; 97(4):1414–21. PMID: [16668565](#)

78. Weiss D. Regulation of flower pigmentation and growth: multiple signaling pathways control anthocyanin synthesis in expanding petals. *Physiologia plantarum*. 2000; 110(2):152–7.
79. Ohto M-a, Onai K, Furukawa Y, Aoki E, Araki T, Nakamura K. Effects of sugar on vegetative development and floral transition in *Arabidopsis*. *Plant Physiology*. 2001; 127(1):252–61. PMID: [11553753](#)
80. Keeling PL, Wood JR, Tyson RH, Bridges IG. Starch biosynthesis in developing wheat grain Evidence against the Direct Involvement of Triose Phosphates in the Metabolic Pathway. *Plant Physiology*. 1988; 87(2):311–9. PMID: [16666140](#)
81. Hii SL, Tan JS, Ling TC, Ariff AB. Pullulanase: role in starch hydrolysis and potential industrial applications. *Enzyme research*. 2012; 2012.
82. Henrissat B, Callebaut I, Fabrega S, Lehn P, Mornon JP, Davies G. Conserved catalytic machinery and the prediction of a common fold for several families of glycosyl hydrolases. *Proceedings of the National Academy of Sciences of the United States of America*. 1995; 92(15):7090–4. PMID: [PMC41477](#).
83. Calviño M, Bruggmann R, Messing J. Screen of genes linked to high-sugar content in stems by comparative genomics. *Rice*. 2008; 1(2):166–76.
84. Tschiersch H, Borisjuk L, Rutten T, Rolletschek H. Gradients of seed photosynthesis and its role for oxygen balancing. *Biosystems*. 2011; 103(2):302–8. doi: [10.1016/j.biosystems.2010.08.007](#) PMID: [20837098](#)
85. Faurobert M, Mihr C, Bertin N, Pawlowski T, Negroni L, Sommerer N, et al. Major proteome variations associated with cherry tomato pericarp development and ripening. *Plant Physiology*. 2007; 143(3):1327–46. PMID: [17208958](#)
86. D'Ambrosio C, Arena S, Rocco M, Verrillo F, Novi G, Viscosi V, et al. Proteomic analysis of apricot fruit during ripening. *Journal of proteomics*. 2013; 78:39–57. doi: [10.1016/j.jprot.2012.11.008](#) PMID: [23178875](#)
87. Terrier N, Ageorges A, Abbal P, Romieu C. Generation of ESTs from grape berry at various developmental stages. *Journal of Plant Physiology*. 2001; 158(12):1575–83.
88. Martínez-Esteso MJ, Sellés-Marchart S, Lijavetzky D, Pedreño MA, Bru-Martínez R. A DIGE-based quantitative proteomic analysis of grape berry flesh development and ripening reveals key events in sugar and organic acid metabolism. *Journal of experimental botany*. 2011; 62(8):2521–69. doi: [10.1093/jxb/erq434](#) PMID: [21576399](#)
89. Marondedze C, Gehring C, Thomas L. Dynamic changes in the date palm fruit proteome during development and ripening. *Horticulture Research*. 2014; 1:14039. doi: [10.1038/hortres.2014.39](#) PMID: [26504545](#)
90. Budde R, Randall DD. Pea leaf mitochondrial pyruvate dehydrogenase complex is inactivated in vivo in a light-dependent manner. *Proceedings of the National Academy of Sciences*. 1990; 87(2):673–6.
91. Sato T, Maekawa S, Yasuda S, Yamaguchi J. Carbon and nitrogen metabolism regulated by the ubiquitin-proteasome system. *Plant signaling & behavior*. 2011; 6(10):1465–8. Epub 2011/09/08. doi: [10.4161/psb.6.10.17343](#) PMID: [21897122](#); PubMed Central PMCID: [PMCPmc3256372](#).
92. Peng M, Hudson D, Schofield A, Tsao R, Yang R, Gu H, et al. Adaptation of *Arabidopsis* to nitrogen limitation involves induction of anthocyanin synthesis which is controlled by the NLA gene. *Journal of experimental botany*. 2008; 59(11):2933–44. Epub 2008/06/17. doi: [10.1093/jxb/ern148](#) PMID: [18552353](#); PubMed Central PMCID: [PMCPmc2504352](#).
93. Ma C, Zhou J, Chen G, Bian Y, Lv D, Li X, et al. iTRAQ-based quantitative proteome and phosphoprotein characterization reveals the central metabolism changes involved in wheat grain development. *BMC genomics*. 2014; 15(1):1029.
94. Zhao X-Q, Shi W-M. Expression analysis of the glutamine synthetase and glutamate synthase gene families in young rice (*Oryza sativa*) seedlings. *Plant science*. 2006; 170(4):748–54.
95. Zhang Z, Zhao H, Tang J, Li Z, Li Z, Chen D, et al. A proteomic study on molecular mechanism of poor grain-filling of rice (*Oryza sativa* L.) inferior spikelets. *PloS one*. 2014; 9(2):e89140. Epub 2014/03/04. doi: [10.1371/journal.pone.0089140](#) PMID: [24586550](#); PubMed Central PMCID: [PMCPmc3931721](#).
96. Paris S, Wessel PM, Dumas R. Overproduction, purification, and characterization of recombinant aspartate semialdehyde dehydrogenase from *Arabidopsis thaliana*. *Protein expression and purification*. 2002; 24(1):99–104. Epub 2002/01/29. doi: [10.1006/prep.2001.1538](#) PMID: [11812229](#).
97. Miron D, Ben-Yaacov S, Reches D, Schupper A, Galili G. Purification and characterization of bifunctional lysine-ketoglutarate reductase/saccharopine dehydrogenase from developing soybean seeds. *Plant physiology*. 2000; 123(2):655–64. Epub 2000/06/20. PMID: [10859195](#); PubMed Central PMCID: [PMCPmc59033](#).
98. Suzuki M, Takahashi M, Tsukamoto T, Watanabe S, Matsuhashi S, Yazaki J, et al. Biosynthesis and secretion of mugineic acid family phytosiderophores in zinc-deficient barley. *The Plant journal: for cell*



- and molecular biology. 2006; 48(1):85–97. Epub 2006/09/16. doi: [10.1111/j.1365-313X.2006.02853.x](https://doi.org/10.1111/j.1365-313X.2006.02853.x) PMID: [16972867](https://pubmed.ncbi.nlm.nih.gov/16972867/).
99. McClung CR, Hsu M, Painter JE, Gagne JM, Karlsberg SD, Salome PA. Integrated temporal regulation of the photorespiratory pathway. Circadian regulation of two Arabidopsis genes encoding serine hydroxymethyltransferase. *Plant physiology*. 2000; 123(1):381–92. Epub 2000/05/12. PMID: [10806255](https://pubmed.ncbi.nlm.nih.gov/10806255/); PubMed Central PMCID: PMC59012.
  100. Cahoon EB, Hall SE, Ripp KG, Ganzke TS, Hitz WD, Coughlan SJ. Metabolic redesign of vitamin E biosynthesis in plants for tocotrienol production and increased antioxidant content. *Nature biotechnology*. 2003; 21(9):1082–7. Epub 2003/08/05. doi: [10.1038/nbt853](https://doi.org/10.1038/nbt853) PMID: [12897790](https://pubmed.ncbi.nlm.nih.gov/12897790/).
  101. Li Y, Wang Z, Sun X, Tang K. Current opinions on the functions of tocopherol based on the genetic manipulation of tocopherol biosynthesis in plants. *Journal of integrative plant biology*. 2008; 50(9):1057–69. Epub 2008/10/11. doi: [10.1111/j.1744-7909.2008.00689.x](https://doi.org/10.1111/j.1744-7909.2008.00689.x) PMID: [18844774](https://pubmed.ncbi.nlm.nih.gov/18844774/).
  102. Munne-Bosch S. Linking tocopherols with cellular signaling in plants. *The New phytologist*. 2005; 166(2):363–6. Epub 2005/04/12. doi: [10.1111/j.1469-8137.2005.01411.x](https://doi.org/10.1111/j.1469-8137.2005.01411.x) PMID: [15819901](https://pubmed.ncbi.nlm.nih.gov/15819901/).
  103. Millar AA, Wrischer M, Kunst L. Accumulation of very-long-chain fatty acids in membrane glycerolipids is associated with dramatic alterations in plant morphology. *The Plant cell*. 1998; 10(11):1889–902. Epub 1998/11/13. PMID: [9811796](https://pubmed.ncbi.nlm.nih.gov/9811796/); PubMed Central PMCID: PMC59012.